

Electrically conductive concrete heated pavement system: Challenges and solution

by

Md Lutfor Rahman

A thesis submitted to the graduate faculty
in partial fulfillment of the requirements for the degree of

MASTER OF SCIENCE

Major: Civil, Construction and Environmental Engineering (Civil Engineering Materials)

Program of Study Committee:
Halil Ceylan, Major Professor
Sunghwan Kim
Peter C. Taylor
Paul G Spry

The student author, whose presentation of the scholarship herein was approved by the program of study committee, is solely responsible for the content of this thesis. The Graduate College will ensure this thesis is globally accessible and will not permit alterations after a degree is conferred.

Iowa State University

Ames, Iowa

2023

Copyright © Md Lutfor Rahman, 2023. All rights reserved.

DEDICATION

To my son, Muttaqi Rahman Imad

TABLE OF CONTENTS

	Page
LIST OF FIGURES	v
LIST OF TABLES.....	vi
ACKNOWLEDGMENTS	vii
ABSTRACT.....	viii
CHAPTER 1. GENERAL INTRODUCTION	1
References.....	4
CHAPTER 2. A REVIEW OF ELECTRICALLY CONDUCTIVE CONCRETE HEATED PAVEMENT SYSTEM TECHNOLOGY: FROM THE LABORATORY TO THE FULL-SCALE IMPLEMENTATION	5
Abstract.....	5
Introduction.....	6
Resistive heating	8
Influencing material-related factors on the performance of ECON HPS	10
Electrically-conductive filler (ECFs)	10
Aggregates.....	13
ECON mixing method.....	14
Dispersion of ECFs.....	14
Electrodes	18
Performance testing of ECON in laboratory	19
Electrical resistivity	19
Resistive heating	20
Application of advanced concrete technology in ECON.....	20
Full-scale implementation of ECON.....	22
Key components	22
System design.....	23
ECON mix design and engineering properties	26
Electrodes	30
Power supply and operation system	31
Construction	33
Performances and costs	34
Application of ECON resistive heating technology in other civil engineering fields	37
Indoor radiant heating.....	37
Ohmic heat curing of concrete	39
Challenges and future recommendations.....	42
Conclusions.....	44
Acknowledgments	45
References.....	45

CHAPTER 3. DEVELOPMENT OF ELECTRICALLY CONDUCTIVE CONCRETE FOR THE CITY OF IOWA CITY SIDEWALK ENHANCEMENT PROJECT	60
Abstract.....	60
Introduction.....	61
Materials and Methods	63
Results and Discussions.....	68
E-1 mixtures	68
E-2 and E-3 mixtures.....	72
Conclusions.....	74
Acknowledgments.....	75
References.....	76
CHAPTER 4. GENERAL CONCLUSIONS.....	79
State of the art and contribution to engineering research	79
Recommendations for Future Studies.....	81

LIST OF FIGURES

	Page
Figure 2-1 Relationship between electrical resistivity and ECF content in ECON	11
Figure 2-2 Design flow chart for ECON heated slab	26
Figure 2-3 Construction steps of ECON HPS: (a) preparation of subgrade and base layer, (b) cutting of trench for placing PVC conduits and placement of dowel baskets, (c) construction of PCC layer, (d) placement of electrodes and wire connections, (e) constructing ECON layer, and (f) backfilling the trench	34
Figure 2-4 Cost breakdown of ECON HPS project in DSM international airport	36
Figure 2-5 Cost breakdown of ECON deck slab Roca spur Bridge Project	37
Figure 2-6 Radiant indoor heating ECON layer structure	38
Figure 3-1 Combined aggregate gradation for (a) 45:10:45 aggregate system (b) 38:19:43 aggregate system	66
Figure 3-2 Relationship between electrical resistivity and cement paste	69
Figure 3-3 Increase in electrical resistivity with time	70
Figure 3-4 Thermal performance of E-1 mixtures.....	71
Figure 3-5 Distribution of CF within the samples (a) Mix-1 (b) Mix-4.....	71
Figure 3-6 Comparison of thermal performance among different mixtures	73

LIST OF TABLES

	Page
Table 2-1 Mix design of ECON.....	10
Table 2-2 Types of ECFs used in the production of ECON and their performances.....	2
Table 2-3 Effects of ECFs on the fresh and hardened properties of concrete.....	9
Table 2-4 Types of ECFs used to produce electrically-conductive cementitious composites in laboratory studies and their performances	11
Table 2-5 Engineering properties of conductive aggregate.....	12
Table 2-6 Mix design and engineering properties of UHPC, LWC, and SCC	21
Table 2-7 ECON layer configuration of full-scale HPS.....	24
Table 2-8 Mix design of ECON for construction of pavements.....	27
Table 2-9 Properties of ECON for road pavement construction	27
Table 2-10 Engineering properties of ECON for Airport pavement construction	28
Table 2-11 Mix design of Test bridge deck for Roca spur Bridge	29
Table 2-12 Properties of ECON for Roca spur bridge deck construction	30
Table 2-13 Electrode configuration, Power supply, and operation system utilized in full-scale ECON HPS	32
Table 2-14 Mix design and engineering properties of ECON used in radiant indoor heating	38
Table 2-15 Mix design and engineering properties of electrically conductive cementitious composites used in ohmic heating.....	40
Table 3-1 – Properties of the aggregates	64
Table 3-2 – Mixture proportions of the E-1 mixtures	64
Table 3-3 – Mixture proportions of the E-2 mixtures	65
Table 3-4 – Mixture proportions of the E-3 mixtures	66

ACKNOWLEDGMENTS

I want to thank all my committee members for their guidance and support throughout this research, especially my advisor, Dr. Halil Ceylan, for his trust and mentorship. In addition, I would also like to acknowledge my loving wife, my supportive parents, and the educational institutions and dedicated teachers who have nurtured my intellect and character. I thank my friends, colleagues, the department faculty, and staff for making my time at Iowa State University a wonderful experience. I want to thank the Iowa Department of Transportation (DOT) and the Iowa Highway Research Board (IHRB) for providing the matching funds for this research, which is sponsored by the Federal Aviation Administration (FAA). I also thank the FAA Air Transportation Center of Excellence for the Partnership to Enhance General Aviation Safety, Accessibility, and Sustainability (PEGASAS). The IHRB technical advisory committee (TAC) members, particularly Mr. Mike Harvey, Director of Iowa DOT's Support Services Office Administrative Services Division, and Iowa DOT electricians, the FAA PEGASAS Technical Monitor for Heated Airport Pavements project, and Mr. Gary L. Mitchell of the American Concrete Pavement Association (ACPA) are gratefully acknowledged for their guidance, support, and direction throughout the research. I sincerely thank other research team members from ISU's Program for Sustainable Pavement Engineering and Research (PROSPER) at the Institute for Transportation for their assistance with the lab and field investigations. Although the Iowa DOT and FAA have sponsored this study, they neither endorse nor reject the findings of this research. The presentation of this information is in the interest of invoking comments from the technical community concerning the results and conclusions of the research. This dissertation does not constitute a standard, specification, or regulation.

ABSTRACT

In regions characterized by harsh winter climates, transportation networks face substantial challenges due to ice and snow accumulation, disrupting air and ground travel. These disruptions can result in significant financial losses the aviation industry and a worrying, problematic increase in weather-related road accidents. Traditional snow and ice removal methods involving mechanical equipment and chemical de-icers are costly and raise ecological concerns by threatening soil and water quality and global food supplies. Heated Pavement Systems (HPS), particularly Electrically Conductive Concrete (ECON) HPS, have emerged as a promising technology, particularly Electrically Conductive Concrete (ECON) HPS, which shows potential in effectively alleviating snow and ice accumulation in critical infrastructure areas such as airports and busy roadways. Despite its promise, the widespread implementation of ECON HPS technology remains limited, warranting a closer investigation into the barriers hindering its adoption. This research paper reviews the existing literature on ECON HPS technology to identify key aspects and challenges. Among the challenges highlighted is the elevated electrical resistivity of ECON during field implementation, increasing its operational costs. Subsequently, the study delves into efforts to produce low-resistivity ECON, presenting findings that provide valuable insights and directions for future research, with the ultimate goal of promoting the widespread adoption of ECON HPS technology and enhancing the resilience of transportation infrastructure in frigid climates.

CHAPTER 1. GENERAL INTRODUCTION

In regions characterized by frigid climatic conditions, the operational efficiency of transportation networks often encounters significant impediments due to the accrual of ice and snow that disrupt air and ground travel [1]. Such disruptions extend beyond mere inconvenience, encompassing substantial financial losses experienced by the aviation industry and problematic escalation in weather-related road accidents [2]. Conventional snow and ice abatement techniques involving mechanical apparatus and chemical de-icers have proven to be fiscally burdensome and engender ecological concerns, jeopardizing soil and water quality and, by extension, the global food supply [2].

The imperative of innovative solutions becomes manifest in confronting these formidable challenges and adapting to evolving climate dynamics. Heated Pavement Systems (HPS) have emerged as a sanguine technology for alleviating snow and ice accumulation in critical infrastructure domains such as airports and high-traffic thoroughfares. While an array of HPS technologies exists, Electrically-Conductive Concrete (ECON) HPS has garnered attention owing to its potential to automate wintertime maintenance operations, obviate the need for deleterious chemicals, and protract the serviceable life of pavements [3].

ECON HPS technology field implementation is still not widespread [2], and the reasons for this lack of use need investigation, so this study intends to review previous research progress on ECON HPS to seek an understanding of the key components of ECON mixture design and ECON HPS technology. Identifying the challenges for full-scale implementation of ECON HPS is the first objective of this study. One of the challenges was ECON's higher electrical resistivity than 1,000 Ω -cm in the case of field implementation. To ensure the economically feasible operation of the ECON, its electrical resistivity should not exceed 1,000 Ω -cm. Since concrete's

electrical resistivity increases with age [3], ensuring lower 28-day electrical resistivity will ensure it does not exceed 1,000 Ω -cm during the pavement's design life. Therefore, the second objective of this study was to produce ECON with 28-day electrical resistivity as low as possible.

This thesis is divided into four chapters. Chapter 1 briefly introduces the thesis and presents its overall organization. Chapter 2 provides a detailed review of the existing literature related to ECON HPS technology to identify the key aspects of its use, the challenges faced by this technology, and how to approach mitigation of those challenges.

Chapter 3 describes a study, part of a full-scale ECON HPS project focusing on producing ECON with the lowest possible electrical resistivity, implementing a self-heating, electrically-conductive concrete heated pavement system for a bus stop enhancement project in Iowa City.

Chapter 2 and Chapter 3 have already been published in peer-reviewed journals and conferences, so those chapters are modified versions taken from those journal and conference publications.

- Chapter 2: Rahman, M.L., Malakooti, A., Ceylan, H., Kim, S. and Taylor, P.C., 2022. A review of electrically conductive concrete heated pavement system technology: From the laboratory to the full-scale implementation. *Construction and Building Materials*, 329, p.127139.
- Chapter 3: M.L. Rahman, A. Malakooti, H. Ceylan, S. Kim, P.C. Taylor, S. Kim, 2023. Development of Electrically Conductive Concrete for the City of Iowa City Sidewalk Enhancement Project, 14th International Symposium on Concrete Roads 2023, Krakow, Poland

Finally, Chapter 4 provides general conclusions summarizing the findings of this study that present directions for future research toward the widespread use of full-scale ECON HPS implementation. **Figure 1-1** is a flow chart representing the thesis structure.

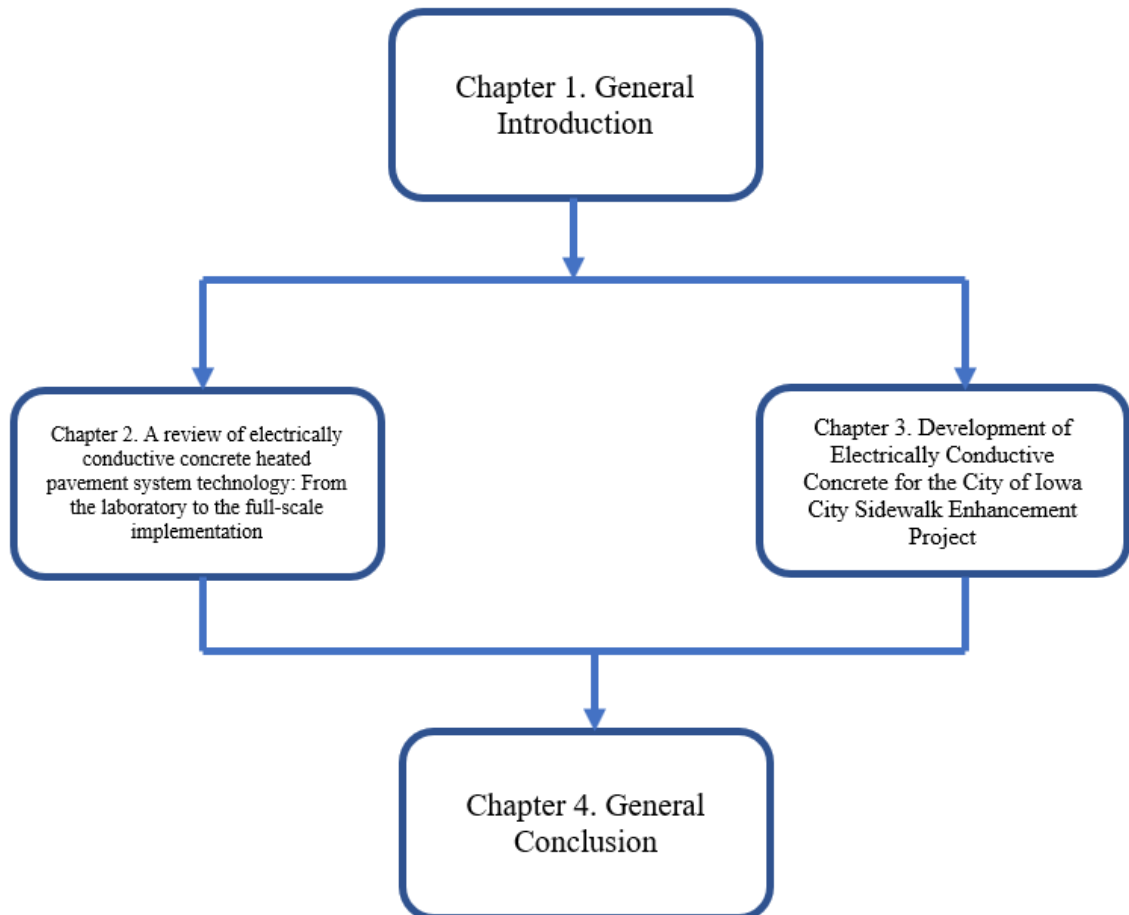


Figure 1-1 Thesis organization

References

- [1] M.L. Rahman, H. Ceylan, S. Kim, Effect of Electrically Conductive Concrete Layer Thickness on Thermal Performance, in: *Int. Airf. Highw. Pavements Conf.*, 2023: pp. 14–23. <https://ascelibrary.org/doi/epdf/10.1061/9780784484906.002>.
- [2] M.L. Rahman, A. Malakooti, H. Ceylan, S. Kim, P.C. Taylor, A review of electrically conductive concrete heated pavement system technology: From the laboratory to the full-scale implementation, *Constr. Build. Mater.* 329 (2022) 127139. <https://doi.org/10.1016/j.conbuildmat.2022.127139>.
- [3] M.L. Rahman, A. Malakooti, H. Ceylan, S. Kim, P.C. Taylor, S. Kim, Identifying the best mixing procedure practice for ready-mix concrete plant production of carbon fibre reinforced electrically conductive concrete, *Int. J. Pavement Eng.* 24 (2023) 1–16. <https://doi.org/10.1080/10298436.2023.2225119>.

CHAPTER 2. A REVIEW OF ELECTRICALLY CONDUCTIVE CONCRETE HEATED PAVEMENT SYSTEM TECHNOLOGY: FROM THE LABORATORY TO THE FULL-SCALE IMPLEMENTATION

Md Lutfor Rahman¹, Amir Malakooti¹, Halil Ceylan², Sunghwan Kim³, Peter C. Taylor⁴

¹Graduate Research Assistant, Department of Civil, Construction and Environmental Engineering (CCEE), Iowa State University, Ames, IA 50011, United States

²Professor of CCEE, ISU Site Director, FAA Partnership to Enhance General Aviation Safety, Accessibility and Sustainability (PEGASAS) Center of Excellence (COE) on General Aviation Director, Program for Sustainable Pavement Engineering and Research (PROSPER), CCEE, Iowa State University, Ames, IA 50011-1066, United States

³Research Scientist, Institute for Transportation, CCEE, Iowa State University, Ames, IA 50011-1066, United States

⁴Research Professor of CCEE, Director of National Concrete Pavement Technology Center, Ames, IA 50010-8664, United States

Modified from a manuscript published in *Construction and Building Materials*

Abstract

Transportation agencies in cold regions often suffer each year economically due to a partial shutdown of their transportation networks during winter storms. Traditional passive ice and snow removal techniques using snowplows, snowblowers, snow shovels, and de-icing chemicals are inefficient and hazardous to the environment and pavement. Adding electrically conductive fillers (ECFs) such as carbon fibers and steel fibers in a standard concrete mixture reduces electrical resistivity and enhances the resistive heating properties of electrically-conductive concrete (ECON). Under the application of electric voltage, the heat from ECON can melt ice and snow accumulated on the pavement. While ECON can be utilized in heated-pavement systems (HPS), field-scale implementation of ECON HPS technology is not yet ubiquitous. This study discusses the challenges that must be overcome to make ECON HPS technology economically attractive to transportation agencies.

Introduction

In cold regions, reduced mobilization capacity of transportation networks often occurs during the winter season because of delays associated with ice and snow accumulation. Since more than three-fifths of the world's airports are in snowy regions, the smooth operation of airline activities is influenced during winter [1]. Flight cancellations or delays of thousands of flights due to ice and snow accumulation on the taxiways, aprons, and runways can occur, and such delays incur substantial revenue loss. For example, the US air transportation sector experiences an estimated revenue loss of \$74.20 per minute per aircraft due to flight delays [2]. Approximately 21% of all accidents that occur on roadways are directly related to weather conditions, and vehicle accidents due to icy, slushy, or snowy pavement account for 29% of such weather-related road accidents and incidents [3]. Motorists and pedestrians experience hardship while traveling in winter [4].

Snow and ice-removal techniques can be subdivided into passive and active categories [5]. Transportation authorities currently utilize passive technologies using mechanical snow-removal equipment and anti-icing or de-icing chemicals to manage snow and ice accumulation; the US consumed 24.5 million metric tons of rock salt in 2019 for roadway de-icing purposes [2]. Anti-icing or de-icing chemicals cause corrosion-related infrastructure deterioration and raise environmental concerns due to soil and water contamination [6]. It is estimated that 50% of the world's arable land will be salinized by 2050, directly affecting the global food supply [7]. Most importantly, dealing with snow and ice accumulation on pavement utilizing traditional snow and ice removal techniques is expensive. For example, the US, China, and the European Union spend 6, 10, and 9 billion dollars yearly on de-icing chemicals and snow removal. In addition, hiring seasonal human resources only during winter is cumbersome for many agencies because not many people are eager to take a job requiring their service for only a quarter of a

fiscal year. In summary, mechanical removal using snow-removal equipment is costly, labor-intensive, and environmentally unfriendly.

Since climate change is making the winter season in some regions even harsher, implementing heated-pavement-system (HPS) technologies to support critical infrastructures such as airports and heavy traffic areas can improve infrastructure resiliency against such climatic conditions [6]. Technologies such as HPS incorporating snow and ice melting techniques fall into the active de-icing categories [5] and include superhydrophobic coating, electrically conductive concrete (ECON) HPS, phase-change material integrated pavement systems, hydronic-HPS, and resistive cable HPS [6,8-10]. Phase Change Material technology negatively affects the mechanical strength of concrete and dynamic elastic modulus and is inapplicable at freezing temperatures [10]. The efficacy of a superhydrophobic coating technique is critically dependent on the spray time and dosage of the polytetrafluoroethylene coating. In addition, the skid resistance of the pavement may become ineffective due to a slight lack of coating [11]. Hydronic-HPS uses glycol through embedded pipes to keep the paving surface temperature above freezing, and any leakage of toxic glycol could become a threat to the environment [12], while the high-power consumption of resistive cable HPS technology obstructs its adoption on a large scale [13].

Among all innovative ice and snow removal technologies, ECON HPS has gained considerable attention because of its favorable results in full-scale implementation projects. ECON is comprised of electrically conductive fillers (ECFs) such as carbon fibers (CFs). The presence of a small dosage of ECFs in concrete increases the electrical conductivity of concrete [14]. Application of an electric potential (voltage) to ECON using embedded electrodes results in heat generation due to inherent resistivity in ECON to current flow. This heat generation acts to

keep the pavement free of ice/snow in winter. The advantage of implementing ECON HPS includes the capability to automate winter maintenance operation, eliminate the use of harmful de-icing chemicals, and extend pavement service life [2,15]. Despite its immense potential, there have been only a few full-scale ECON HPS implementation projects.

This study aims to identify the challenges in the widespread adoption of ECON HPS technology by analyzing influential construction material-related factors that affect ECON performance and critical components of ECON HPS technology.

Resistive heating

Malakooti et al. developed the theoretical formulation for ECON HPS performance presented herein [2]. According to Ohm's first law, under the application of electric current, under steady-state conditions, voltage has a linear relationship to the electrical resistance of the material, as shown in Equation (1).

$$V = I.R \tag{1}$$

Where I is the electric current, V and R are the applied voltage and the material's resistance. Resistance (R) can also be calculated using Equation (2). Electrical resistivity (ρ) is a material property normalized by the specimen's dimensions [16].

$$\rho = \frac{R.A}{L} \tag{2}$$

In Equation 2, A is the conductive cross-sectional area in the direction of current flow, and L is the distance between electrodes. The applied electrical energy (E) is converted into thermal energy (Q) through the resistive heating mechanism [17]. As shown in Equation (3), electrical energy is a product of electric power (P) and operational time (Δt) [18].

$$E = P \cdot \Delta t = \frac{V^2}{R} \cdot \Delta t = \frac{V^2 \cdot A}{\rho \cdot L} \cdot \Delta t \quad (3)$$

The generated thermal energy in a material is a function of the mass (m), the change in temperature of the material (ΔT), and the specific heat capacity (C), as shown in Equation (4) [19].

$$Q = m \cdot C \cdot \Delta T \quad (4)$$

Equating electrical and thermal energy results in Equation (5) [2].

$$\frac{\Delta T}{\Delta t} = \frac{V^2 \cdot A}{\rho \cdot L \cdot m \cdot C} \quad (5)$$

Equation (5) indicates that it is conceivable that higher applied voltage (V) and lower electrical resistivity (ρ) of ECON produce better thermal performance if other material properties remain constant [2]. It is worth mentioning that PCC is considered a non-conductive material since its electrical resistivity in dry conditions varies between 6.54×10^5 and $11.4 \times 10^5 \Omega\text{-cm}$ [20], and to prevent ice formation or to melt the accumulated ice, ECON with a resistivity of less than 1,000 $\Omega\text{-cm}$ is required [15,21,22]. The electrical conductivity of standard PCC can be enhanced by incorporating ECFs into the PCC mixture [23]. Xie et al. suggest ranges of some mix proportioning parameters, as shown in **Table 2-1**, to produce ECON with an electrical resistivity value between 1 and 100 $\Omega\text{-cm}$ and a 30 to 50 MPa compressive strength.

Table 2-1 Mix design of ECON

Items	Material Range [4]
ECFs	0 to 8 vol.%
Water to cementitious material ratio	0.35 to 0.75
Fine aggregate/cement ratio	0 to 2 by wt.
Coarse aggregate/cement ratio	0 to 2 by wt.
Dispersant/cement ratio	0.1 to 5 wt.%

The electrical resistivity of ECON is a function of temperature, which decreases with increasing temperature because of a negative temperature coefficient [25]. However, some researchers observed an increase in the electrical resistivity of ECON after a certain voltage level because of a positive temperature coefficient [26,27].

Influencing material-related factors on the performance of ECON HPS

Electrically-conductive filler (ECFs)

Electrically-conductive filler has the lowest electrical resistivity among the constituent materials of ECON [28], so its role is pivotal in increasing the conductivity of the concrete. As shown in **Figure 2-1**, the resistivity of ECON decreases with the addition of electrically-conductive fillers. This generalized behavior can be divided into three subsections (AB, BC, and CD). ECON's electrical resistivity decrease rate increases abruptly in the BC zone, known as the percolation zone. Beyond the BC zone, increasing the electrically-conductive filler content does not help improve electrical conductivity but decreases ECON's workability and mechanical strength. Moreover, since excess use of more conductive filler than necessary is economically inefficient [9], the optimum ECON conductive filler content should be at point C in **Figure 2-1** to ensure satisfactory resistive-heating performance.

Determining the percolation threshold requires several trials in the laboratory using an increasing dosage of conductive filler. Researchers have also developed mathematical models to calculate the optimum dosage of ECFs required to increase the electrical conductivity of ECON.

Equations (6) and (7) provide a mathematical model for determining the content of conductive filler (x) needed in the mix to ensure a better connection (y) between the fillers and, as a result, better electrical conductivity.

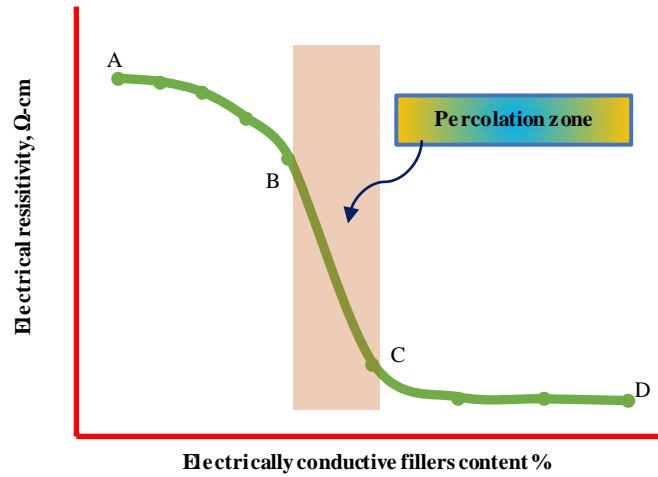


Figure 2-1 Relationship between electrical resistivity and ECF content in ECON

$$x = \frac{\sum_{i=1}^n V_i}{V_s} \quad (6)$$

$$y = \frac{\sum_{k=1}^c V_k}{\sum_{i=1}^n V_i} \quad (7)$$

Where V_i and V_s denote the respective volumes of individual ECFs and ECON, individually connected ECFs tend to cluster, and the total amount of the connected ECFs are represented respectively by V_k and c . A y value of 1 will ensure all fillers contact one another in the ECON mix. Tian et al. reported that this numerical approach could accurately estimate the percolation threshold of any ECF [29].

Researchers have incorporated ECFs in ECON in either single-phase form or a combination of two or more ECFs. Carbon fibers, steel fibers, graphite, carbon black, steel

shavings, iron-particle-contained Nano-graphite, carbon nanotubes, carbon nanofibers, nickel particles, CuSO_4 , FeSO_4 , iron powder, expanded graphite, and waste wire erosion are some examples of ECFs utilized so far. **Table 2-2** summarizes various types of ECFs used in the production of ECON and their performances, and Table 3 illustrates the effects of various ECFs on the fresh and hardened properties of concrete.

Single-doped ECFs

Carbon fibers (CFs)

As shown in **Table 2-2**, among the types of ECFs used in laboratory-scale preparation of ECON, CFs dominate. CFs offer good electrical and thermal conductivity and have low thermal expansion coefficients, high specific strengths, fatigue resistance, corrosion resistance, and high elastic moduli, all significant advantages. Polyacrylonitrile-based CFs perform superior to pitch-based CFs because their electrical conductivity is seven times better [30]. A high aspect ratio (length to diameter) of CFs increases conductivity. However, since the dispersion of CFs into a concrete matrix becomes a challenge due to reduced workability, CFs with aspect ratios ranging from 400 to 900 are suggested for ECON production [31,32]. Although the electrical conductivity and mechanical strength of ECON increase with increasing dosage of CFs, above a specific dosage limit of CFs in ECON, electrical conductivity is not significantly improved. Mechanical strength becomes negatively impacted due to poor workability caused by fiber entanglement [33]. **Table 2-3** represents the influence of CFs and other ECFs on ECON's fresh and hardened properties. While in laboratory studies, a dosage of 0.5 vol.% to 0.75 vol.% of CFs in ECON is suggested for achieving a desirable resistive heating performance [32], a higher dosage of CFs is seen as necessary during ECON full-scale field implementation to accommodate CF loss to the air while mixing with concrete [34].

Steel fibers (StF)

Incorporating StF ensures improved elastic modulus and flexural strength of ECON [35]. While StF (8 μm -diameter) doped ECON can achieve electrical resistivity as low as 0.85 $\Omega\text{-cm}$ [36], a corrosion layer that develops around steel fiber increases the resistivity of ECON with time, so a corrosion inhibitor admixture is required in the concrete matrix if StF is utilized in the production of ECON [30,36]. High dosages, corrosion, and prohibition of StF in airports limit their use in ECON-based HPS [32]. If necessary, a low dosage of StF can be combined with other ECFs [30].

Graphite

Good electrical resistivity ranging from 10^{-1} and 10^{-5} $\Omega\text{-cm}$ and increased durability of concrete [41] make graphite an excellent candidate for use in ECON. Among various particle sizes of graphite, particles passing 200 mesh provide the best electrical performance [30], and in order to achieve the desired level of electrical conductivity, the matrix's graphite content should be high. In addition, due to graphite's greater water contact angle than that of cement, graphite particles show less hydrophilic behavior, so the incorporation of graphite in a concrete mix demands increased water to achieve the desired workability, explaining why the incorporation of graphite results in lower compressive strength of ECON [51]. In summary, incorporating graphite only as a secondary filler is preferred since the graphite dosage in the mix is limited, limiting its adverse effect on the mechanical properties of ECON [30].

Carbon black (CB)

Incorporation of CB can enhance ECON density and increase ECON compressive strength and toughness [42,52]. Compared to fibers, particle fillers like CB require a higher dosage [35]. The use of CB in ECON decreases workability, fresh concrete unit weight, and

compressive strength but increases durability [41]. Like graphite, CB is also widely utilized as a secondary filler, as shown in **Table 2-2**.

Steel shavings (SSh)

SSh is waste material and byproduct of the steel-manufacturing industry. Although incorporating SSh increases ECON electrical conductivity, that increase has been found to be unsuitable for use in HPS. Mechanical strength also decreases if SSh is incorporated in ECON [21], and poor consistency with respect to composition and size because of divergence in SSh' sources, oil contamination, and dispersion difficulty limit their use in ECON HPS.

Iron particle contained composite Nano-graphite (ING)

In a search for cheaper alternatives, ING was tried for producing ECON with low resistivity, but ING not only decreased the mechanical strength of ECON, but even as much as with 5 wt.% ING in the concrete mix did not result in suitable electrical resistivity of the produced mix [48].

Table 2-2 Types of ECFs used in the production of ECON and their performances

ECFs type & Concentration	Mix proportion		Mechanical properties & workability	Electrical resistivity (Ω-cm)	Heating performance	References
CFs-1 vol.%	w/cm = 0.42 FA/c = 1.42 CA/c = 1.25	IA/c = 0.62 SR = 43% Dispersant/c = 0.2wt.%	$\sigma_c = 39$ MPa $\sigma_f = 47.6$ MPa Slump = 38 mm	115	Not Available	[5]
CFs -0.74 vol.%	FAh = 20 wt.% w/cm = 0.45 FA/c = 2.2 CA/c = 3.5	SR = 38.6%, Dispersant/c = 0.4 wt.% SP = 0.7 wt.%	$\sigma_c = 40$ MPa $\sigma_f = 4$ to 5 MPa	50	2.5 cm thick ice was completely melted in 35 min (Under 80 C and 11A)	[6]
CFs (Recycled)-0.407 vol.%	w/cm = 0.14 FA/c = 1.45 LF/C = 0.25	SP = 3.7 wt.% NS = 7.1 wt.% Mixing Method: Wet	Not Available	Not Available	0.083 ⁰ C/min at room temperature	[7]
CFs-2 vol.%. .	SiF = 5 wt.% w/cm = 0.47 FA/c = 2.3	CA/c = 1.60 SR = 59% SP = 1 wt.%	$\sigma_c = 49.02$ MPa $\sigma_f = 11.73$ MPa	Not Available	0.1085 ⁰ C/min	[8]

Table 2-2 Continued

ECFs type & Concentration	Mix proportion		Mechanical properties & workability	Electrical resistivity (Ω-cm)	Heating performance	References
CFs (Recycled)-0.2 to 0.8 vol.%	w/cm = 0.14 FA/c = 1.45 LF/C = 0.275	SP = 3.75 wt.% NS = 7.125 wt.% Mixing Method: Wet	$\sigma_c = 80$ MPa $\sigma_f = 16$ MPa	60 to 300	Not Available	[9]
CFs-2 wt.% (Oxidation treatment of CF)	SiF = 10 wt.% w/cm = 0.5 FA/c = 0.75	CA/c = 1.125 SR = 40% SP = 2.1 wt.%	Not Available	44 to 48	Not Available	[10]
Graphite -7 vol.% of FA	w/cm = 0.57 FA/c = 1.71 CA/C = 3.41 SR = 0.33 Mixing Method: Dry		Air content = 1.5% Fresh concrete unit weight = 2325 kg/m ³ Water absorption = 1% $\sigma_c =$ Nearly 24 MPa $\sigma_t =$ Nearly 3.2 MPa	500	Not Available	[11]
CB-0.83 vol.% + CFs-0.49 vol.%	FAh = 26.5wt.% w/cm = 0.41 FA/c = 1.40 LWA/c = 1.09	SR = 39 vol.% Dispersant/c = 0.2wt.% SP = 1.26 wt.% Mixing Method: Wet	$\sigma_c = 33.8$ MPa $\sigma_f =$ More than 5 MPa	63.2	Not Available	[12]

Table 2-2 Continued

ECFs type & Concentration	Mix proportion		Mechanical properties & workability	Electrical resistivity (Ω-cm)	Heating performance	References
CB-6 wt.% + CFs-1 vol.%	w/(c + CB) = 0.48 FA/c = 2 CA/c = 2	SR = 50% SP = 1.75 wt.% Dispersant/c = 0.2wt.%	Slump = 45 mm $\sigma_c = 47.82$ MPa $\sigma_f = 8.62$ MPa	Cylinder: 80.08 Slab: 357	From -10 ⁰ C to 32 ⁰ C in 120 minutes (Under 120 V)	[13.14]
CB-6 wt.% + CFs-0.2 vol.% + WWE-1.5 vol.%	w/(c + CB) = 0.48 FA/c = 2 CA/c = 2	SR = 50% SP = 1.60 wt.% Dispersant/c = 0.2wt.%	Slump = 45 mm $\sigma_c = 39.52$ MPa $\sigma_f = 7.21$ MPa	Cylinder: 97.74 Slab: 270	From -10 ⁰ C to 37.3 ⁰ C in 120 minutes (Under 120 V)	
CB (Recycled)-20 wt.% + CFs-0.5 vol.%	w/(c + CB) = 0.48 FA/c = 2 CA/c = 1.58 SR = 56%	SP = 1.25 wt.% Dispersant/c = 0.2wt.% Mixing Method: CB- Dry, CF-wet	Slump = 70 mm $\sigma_c = 30.5$ MPa $\sigma_f = 6.23$ MPa	Cylinder = 132 slab = 21	From -12 ⁰ C to 10 ⁰ C in 105 minutes (Under 60 V)	[15]
StF-3 vol.% + Steel Powder- 5.8 vol.%	w/cm = 0.4 FA/c = 1.9 CA/c = 2.5	SR = 43% SP = 1 wt.%	$\sigma_c = 40$ MPa	500	From -14.6 ⁰ C to 1.3 ⁰ C in 150 minutes (Under 44 V)	[16]
StF-2 wt.% of CA + Graphite-10 wt.% of Fine Aggregate	FA/c = 1.55 CA/c = 2.33 SR = 40%		Not Available	45,000	Not Available	[17]

Table 2-2 Continued

ECFs type & Concentration	Mix proportion		Mechanical properties & workability	Electrical resistivity (Ω-cm)	Heating performance	References
StF-1 vol.% + CFs-0.4 vol.% + Graphite-4 wt.%	w/cm = 0.44 FA/c = 1.30	CA/c = 1.80 SR = 42%	$\sigma_c = 41.2$ MPa	322	From -13.8 ^o C to 8 ^o C in 120 minutes (Under 44 V)	[18]
Graphite-10 wt.% + Stainless StF (in two layers)	SiF =15 wt.% w/cm = 0.5 FA/c = 1.18		Not Available	40	Not Available	[19]
ING-3 wt.%	w/cm = 0.43 FA/c = 1.31 CA/c = 2.38	SR = 35% SP = 0.7 wt.% Mixing method: Wet	$\sigma_c = 28.2$ MPa	5,00,000	Not Available	[20]

Table 2-2 Continued

ECFs type & Concentration	Mix proportion		Mechanical properties & workability	Electrical resistivity (Ω -cm)	Heating performance	References
Graphite-4 wt. %	SS = 25 wt. % GGBS = 15 wt. % w/cm = 0.46	FA/c = 3.28 CA/c = 4.82 SP = 0.53 wt. % SR = 40.44 %	$\sigma_c = 41.5$ MPa $\sigma_f = 3.5$ MPa	1,054	Not Available	[21]
Graphite-4 wt. %	SS = 20 wt. % GGBS = 15 wt. % w/cm = 0.55 FA/c = 3.02	CA/c = 4.45 SP = 0.48 wt. % SR = 40.44 %	$\sigma_c = 36$ MPa $\sigma_f = 3.4$ MPa	7,779	Not Available	[22]
<p>*w/cm = Water to cementitious material ratio CA/c = Coarse aggregate to cement ratio FA/c = Fine aggregate to cement ratio IA/c = Intermediate aggregate to cement ratio</p> <p>SP = Super plasticizer LF/c = Limestone Filler to cement ratio FAh = Fly ash SiF = Silica fume</p> <p>σ_c = Compressive strength σ_t = Splitting tensile strength σ_f = Flexural strength</p> <p>Wt. % = Otherwise mentioned, percentage weight by cement vol% = Otherwise mentioned, percentage volume of concrete SR = Sand ratio</p> <p>SS = Steel slag GGBS = Ground granulated blast furnace slag</p>						

Carbon Nano-Tubes (CNTs)

Because of their lower resistivity, $10^{-7} \Omega\text{-cm}$ [56], and higher packing density, 50-150 kg/m^3 [56], Nano-materials like CNTs have been gaining popularity [57]. Both single-walled and multi-walled CNTs (MWCNTs) are one-dimensional materials [58] widely used to enhance the electrical conductivity of cementitious sensors [59–67]. The good mechanical properties, low resistivity, and satisfactory heating performance of CNTs-based ECON support their utilization in ECON HPS [68–70]. While the percolation threshold for CNTs in cementitious composites is 1 wt.% [71], the large specific surface area and Van der Waals force of CNTs results in poor mechanical strength and workability of CNTs-based ECON due to fiber agglomeration at high dosage [53]. High cost is another drawback of incorporating CNTs in ECON [72]. **Table 2-4** presents the mix proportioning and performance of CNTs-based electrically-conductive cementitious materials and other ECFs-based cementitious composites.

Carbon Nano-Fibers (CNFs)

CNFs have electrical resistivity as low as $0.78 \Omega\text{-cm}$ [29], but it is difficult to disperse them uniformly in a cement matrix because they have a high specific surface area, $40 \text{ m}^2/\text{g}$ [29], making them likely to agglomerate. CNFs' poor dispersion also leads to internal defects that weaken the ECON mechanical strength. The percolation threshold for CNFs in cementitious composites is 0.5 wt.% [71].

Graphene or Graphene Nano-Platelets (GNP)

GNP is a 2D Nano-carbon material with high mechanical strength and electrical conductivity. The percolation threshold for GNP in ECON is 2 vol.% [73,74]. Reduction in the porosity of cementitious matrix due to the incorporation of graphene [75] contributes to improved elastic modulus and mechanical strength of ECON [74]. GNP also improves ECON's thermal diffusivity and thermal stability [72].

Hybrid ECFs

High dosage requirements, high cost, and poor workability drive the research community to combine two or more ECFs in the ECON mixture to achieve low electrical resistivity. For example, a combination of CFs, StF, and graphite assisted in lowering the CFs dosage in the ECON mixture and solving problems associated with using StF only in ECON production. Although micro-scale ECFs are most effective in increasing the electrical conductivity of ECON [76], hybridization of micro-scale ECFs with Nano-scale assists in ensuring better electrical connectivity within the ECON mixture matrix since Nano-materials fill the spaces that micro-materials cannot reach. For example, combining CNFs and CFs improves the ECON mixture's heating performance compared to using CFs only [77]. **Table 2-2** lists the hybrid ECFs that have been utilized to produce ECON

Table 2-3 Effects of ECFs on the fresh and hardened properties of concrete

ECFs	Compressive Strength		Flexural Strength		Workability	Durability
Carbon fibers	↑ Up to 0.5 vol.% [23]	↓ Beyond 0.5 vol.% [23]	↑ Up to 0.75 wt.% [24]	↓ Beyond 0.75 wt.% [24]	↓ [4]	Research Gap
Steel fibers	↑ [25]		↑ [25]		Research Gap	Research Gap
Steel shavings	↓ [11]		↓ [11]		↑ [11]	↑ [11]
Graphite	↓ [11]		↓ [11]		↓ [11]	↓ [11]
Carbon Nanotubes	↑ Up to 0.1 wt.% [26]	↓ Beyond 0.1 wt.% [26]	↑ Up to 0.1 wt.% [27]	↓ Beyond 0.1 wt.% [27]	↓ [28]	Research Gap
Carbon Nanofibers	↓ [25]		Research Gap		↓ [29]	Research Gap

Table 2-3 Continued

ECFs	Compressive Strength		Flexural Strength	Workability	Durability
Carbon black	↓ [11]		↓ [11]	↓ [11]	↓ [11]
Graphene Nanoplatelets	↑ Up to 2 vol.% [25]	↓ Beyond 2 vol.% [25]	Research Gap	↓ [25]	Research Gap
Nano SiO ₂	↑ Up to 0.1 wt.% [25]	↓ Beyond 0.1 wt.% [25]	Research Gap	Research Gap	Research Gap
Nano TiO ₂	↑ Up to 0.5 wt.% [25]	↓ Beyond 0.5 wt.% [25]	Research Gap	Research Gap	Research Gap

Table 2-4 Types of ECFs used to produce electrically-conductive cementitious composites in laboratory studies and their performances

ECFs type & Concentration	Mechanical properties & workability	Electrical resistivity (Ω-cm)	Heating performance	References
CNTs Less than 0.6 wt.% of cement	$\sigma_c = 35$ MPa	145.2	2.41 ⁰ C/min	[28]
CNTs 0.5 wt.% of cement	$\sigma_c = 50$ MPa	Not Available	0.142 ⁰ C/min (Under 120 V)	[30]
Iron Powder 20 wt.% of cement	Slump = 119 mm $\sigma_c = 40$ MPa $\sigma_t = 2.70$ MPa	2,500	0.48 ⁰ C/min (Under 60 V)	[31]
FeSO ₄ -9.1%	$\sigma_c = 32.4$ MPa	9,329	0.164 ⁰ C/min (Under 30 V)	[32]
CuSO ₄ 4.8%	$\sigma_c = 32.4$ MPa	12,779	0.09 ⁰ C/min (Under 30 V)	
CFs-0.75 vol.% of mortar + CNF-0.3 vol.% of cement paste	Not Available	Not Available	0.39 ⁰ C/min	[33]
GNP-2 vol.%	Not Available	100	Not Available	[34]
Nickel Particles-Type 287-12 vol.% of mortar	Not Available	35	100 ⁰ C/min (Under DC-20 V)	[35]
Expanded graphite- 9 wt.%	$\sigma_c = 11$ MPa	100	8.82 ⁰ C/min (Under 15 V) Power input = 950 W/m ²	[36]

Table 2-5 Engineering properties of conductive aggregate

Items	References			
	[37]	[38]		[39]
Conductive filler	Graphite Powder-10 wt.% of clay	CF-1 vol.%	CF-0.5 vol.% + CB-2.0 wt.% of cement	Marconite- 1 wt.% of total raw materials
Specific gravity (kg/m ³)	1,760	Not Available	Not Available	Not Available
Water absorption (%)	15.20	13.08	24.41	12.93
Electrical resistivity (Ω -cm)	Less than 500	340	734	3,920
Crushing Strength (MPa)	Not Available	1.57	0.95	11.12

Aggregates

Both the quantity and quality of the cement paste impact the performance of concrete. Aggregates occupy 50 to 70% of the volume of concrete, and the volume of voids in the combined aggregate system determines the cement paste requirements in a conventional concrete mix [78]. Cement paste is more electrically conductive than aggregates [79]. Since it is impossible to form a continuous conductive path by individually connected ECFs, cement paste can act as a conductive component in places without conductive filler, so the aggregate system plays a vital role in ECON's overall electrical conductivity and resistive heating performance. There are contradictory opinions regarding the effect of cement: coarse aggregate: fine aggregate ratios on the electrical resistivity of ECON. According to Sassani et al., the electrical resistivity of ECON increases and mechanical strength decreases with increasing coarse-to-fine aggregate volume ratio [80], so the content of coarse aggregates must be kept as low as possible to achieve ECON with low electrical resistivity [81]. On the other hand, Hou et al. suggest that an increase of coarse aggregate increases the ECON electrical conductivity by ensuring more accumulation of ECFs in the matrix. In addition, the electrical conductivity of ECON decreases when the fine aggregate-to-cement ratio rises above 2 [82]. The particle-size distribution of sand also influences the electrical resistivity behavior of cementitious materials. Due to its smaller packing density, finer sand provides less electrically-conductive concrete than standard-sized sand [83]. In addition, since a sand ratio too high or too low fails to provide desirable electrical resistivity, a suitable sand ratio should be determined for each mix [30].

Conventional coarse aggregates are electrically non-conductive, with their electrical resistivity varying between 3×10^4 to $15 \times 10^4 \Omega\text{-cm}$ [21], and replacing conventional aggregates with conductive aggregates can assist in achieving the desired resistivity for ECON.

Contradictory observations can be found in the literature related to the effectiveness of

conductive aggregates in achieving desirable ECON conductivity. Some suggest that adding conductive aggregate alone will assist in achieving resistivity as low as 10 to 30 Ω -cm [23], while others think that incorporating conductive filler along with conductive aggregate is necessary to achieve the desired conductivity of ECON [84]. There are also some challenges in incorporating conductive aggregate in the mixture. First, conductive aggregates should have a similar shape to the natural coarse aggregates, which is sometimes difficult to achieve [85]. Second, since conductive aggregate requires a high-water content during mixing, the compressive strength of ECON can decrease to below 25 MPa [23]. **Table 2-5** lists the basic properties of conductive aggregates used by researchers.

ECON mixing method

Proper mixing is essential to achieve uniform distribution of ECFs in an ECON mixture, and the mixing method of ECON is sensitive to the particle size of the materials used. Finer ECFs absorb more water and are more difficult to mix than coarser ECFs [90]. There is still a lack of systematic guidance or specification for ECON mixing methods. Some researchers have proposed wet mixing -adding ECFs after mixing aggregate, cement, and water - to achieve better dispersion of ECFs, workability, and mechanical strength [39,91]. In contrast, others suggest incorporating conductive filler into the mix before adding water, commonly known as dry mixing. While dry mixing is preferred for achieving a uniform distribution of carbon-based materials [73], it may lead to loss and degradation, especially of fiber-type ECFs [9].

Dispersion of ECFs

Typical ECFs used in ECON are mainly micron or nano-scale materials. Particle attraction force increases with increasing surface area, resulting in difficulty with dispersion within the mix [14], and the hydrophobicity of some conductive filler obstructs their dispersion

within the ECON matrix [92]. The porosity of an ECON matrix increases with conductive filler entanglement, resulting in poor mechanical properties, electrical properties, and structural integrity [9]. Conductive filler dispersion uniformity is vital for ECON construction since it directly affects resistivity, heating performance, and operational cost [41]. Moreover, a uniform dispersion ensures uniform heating of ECON since the temperature distribution throughout the ECON slab is just as important as the temperature rate of increase [37].

Dispersion techniques

Mechanical methods

While ultrasonication with surfactant in an aqueous solution ensures uniform dispersion of ECFs [40,94,95], identifying appropriate ultrasonic energy and frequency is necessary to achieve the desired electrical conductivity and mechanical strength of ECON for HPS. Because excessive ultrasonic energy leads to a high number of microbubbles on the surface of ECFs, especially for micro-fibers, it can lead to stress concentration and a corresponding decrease in mechanical strength of ECON [53]. High shear mixing and ball milling can also effectively separate ECFs from one another and ensure appropriate dispersion. Meanwhile, since the fragmentation of fiber-type ECFs can occur, possibly leading to the poor electrical conductivity of ECON because of the resulting reduced aspect ratio of the ECFs, the mechanical dispersion method of ECFs is appropriate only for nano-scale fillers [14].

Use of dispersion materials

Since mechanical methods of filler dispersion are not appropriate for all ECFs, adding dispersion material may be a viable alternative. An ideal dispersion material should offer good compatibility with the other materials used in the production of ECON and impart no or at least negligible adverse effects on cement hydration, fresh concrete properties, and hardened concrete

engineering properties [96]. Two types of dispersion materials have been used in the development of ECON: mineral admixtures and chemical admixtures.

Chemical admixtures

Rheology plays a vital role in distributing conductive filler, electron movement, and the generation of conductive paths in an ECON mixture [97]. Chemical admixtures, e.g., fiber dispersive agents and high-range water reducers (HRWR), can assist in dispersing ECFs into the mixture. Fiber dispersive agents ensure uniform distribution of conductive agents, resulting in lower electrical resistivity and improved compressive strength [30,94]. Carboxymethyl cellulose (CMC) is more effective in achieving uniform dispersion of carbonaceous ECFs than hydroxyethyl cellulose, hydroxypropyl cellulose, or polyvinyl pyrrolidone [94]. Adding water-reducing admixtures to the ECON mix becomes necessary to maintain the desired workability. While HRWR usually favors the strength and conductivity of electrically conductive cementitious materials [53], increases slump, and ensures better bonding of the electrodes with the concrete, its use requires extra caution because a slight overdosage of HRWR may cause bleeding and segregation [98]. Polycarboxylate-based HRWR is the most common additive used in the production of ECON, and Naphthalene-based HRWR is another type utilized [45]. Among other chemical admixtures, sodium dodecyl sulfate and sodium dodecylbenzene sulfonate can help achieve a uniform dispersion of conductive filler [96]. As mentioned earlier in section 3.4.1.2, compatibility between the chemical admixtures is critical since it affects the performance of ECON.

Mineral admixtures

Incorporating supplementary cementitious materials (SCM) such as slag, silica fume, and fly ash reduces the pore structure. Although some researchers suggest using SCM in ECON because they obtained significantly lower electrical resistivity, others found that they negatively

affected ECON's electrical conductivity and mechanical properties [90,95,99,100]. The addition of SCM increased the standard deviation of ECON samples' electrical resistivity and mechanical properties. Mineral admixtures have also adversely affected ECON workability [9]. The electrical conductivity of ECON with SCM increases much faster than that of standard concrete of a later age. Since this effect is more prominent for silica fume than fly ash [101], a small amount of SCM can be added for durability [100,102]. As a result, a balance must be achieved when using SCM in ECON to ensure desirable electrical resistivity, durability, and mechanical performance.

Dispersion evaluation

Measuring the actual content of ECFs in a hardened concrete sample can be achieved by dissolving ECON in Hydrochloric acid [9]. In addition, the coefficient of weight variation (CV) technique shown in Equation (8) can directly and quantitatively estimate the fiber uniformity for fresh cementitious materials, where a lower CV value indicates a better conductive filler distribution [94].

$$CV = \frac{\sqrt{\sum_{i=1}^n (m_i - \bar{m})^2 / (n - 1)}}{\bar{m}} \times 100\% \quad (8)$$

Where m_i expresses the conductive filler mass at the i th location, \bar{m} is the average mass of carbon fiber, and n indicates the quantity of the total mix. Measurement of electrical resistance of ECON samples, observation of fresh mixture, microstructure observation, etc., are additional techniques that can be used to evaluate the dispersion of ECFs throughout the ECON sample [14].

Electrodes

Electrodes, the means for applying an electric potential to ECON, should exhibit high electrical conductivity. ECON temperature increases with increased surface contact area between the electrode and ECON [2]. Therefore, adequate bonding between ECON and the electrodes should be established [13,98]. Steel reinforcing bars, steel mesh, stainless galvanized steel sheet, carbon steel plates, stainless steel wire mesh, perforated galvanized steel, steel sheets with rhomboidal grid, aluminum mesh, and copper mesh all have been utilized as electrodes in ECON HPS. While perforated angle electrodes are superior to bar-type electrodes from the perspective of better heating performance [103], using angle electrodes decreases the durability of ECON HPS due to stress concentration at the angled edge, increasing crack-formation potential [13]. Perforated electrodes with larger gaps than the maximum aggregate size can ensure better bonding with concrete and better heating performance [15,23]. Flat bars exhibited the highest power density and temperature increase rate among smooth flat, circular solid, and circular hollow-type electrodes [34]. Instead of unnecessarily spending resources, after producing laboratory-scale ECON samples to compare the heating performance between electrodes with different materials, shapes, and sizes, Malakooti et al. suggest testing electrodes in water [2]. Flat-bar orientation (horizontal or vertical) in the ECON layer did not affect the heating performance of HPS [2]. Although a higher electrode cross-sectional area will ensure superior thermal performance [104], smaller-diameter and flat-bar electrodes are more cost-effective when considering initial cost and relative temperature increase rate [2]. Testing electrodes in water is a non-destructive, fast, cost-effective, and repeatable method for determining performance and identifying favorable electrode sizes [2].

The optimum electrode spacing in an ECON slab depends on the electrical resistivity of ECON, ECON thickness, and the electrical power necessary to prevent ice or snow formation at

a particular location [8,15]. Decreasing electrode spacing will increase the heating performance of the ECON slab [13,98]. Electrodes can be embedded in the slab using one of two configurations: left-right (L-R) or top-bottom (T-B). Contradictory findings regarding the resistive heating performance of ECON having a T-B configuration are reported, but the construction process complexity prohibits the utilization of T-B arrangements in ECON field construction [105].

Reinforcing bars are placed in the concrete pavement slab as longitudinal or transverse bars. The effect of reinforcing bars on resistivity and heating performance requires evaluation concerning suppressing stresses due to temperature and shrinkage. A reinforcing bar was detrimental to ECON's heating efficiency since the electric current tends to pass through the reinforcing bars rather than the ECON [44], so ECON HPS with reinforcing bars does not provide a significant temperature increase [37]. Moreover, steel reinforcing bars are susceptible to corrosion, affecting the electrode surface contact area with ECON and negatively impacting the temperature increase in HPS [2,98].

Performance testing of ECON in laboratory

Since mechanical strength testing of ECON is similar to that for conventional concrete, only electrical property testing will be discussed here.

Electrical resistivity

Measurement techniques can affect the electrical resistivity value of ECON [106], especially at low ECF content [107]. The two-electrode method and the Wenner probe (four-electrode) method are widely used to measure the electrical resistivity of ECON, with a contact resistance phenomenon in the case of the two-electrode method. While the two-electrode method thus reflects a less accurate electrical resistivity measurement method than the four-electrode method [106], the greater simplicity and convenience of the two-electrode testing method has

resulted in the research community utilizing this technique [14]. The electrical resistivity of ECON is a function of the applied electric voltage [106]. Although electrical resistivity values reported in Tables **Table 2-2** and **Table 2-3** were tested for various electric voltage levels, a standard electric voltage level was used to report the electrical resistivity of the ECON produced in the laboratory. A 12V applied voltage provided accurate electrical resistivity measurements for the four-electrode method, while 16V was acceptable for the two-electrode method [106]. Although cylindrical shape samples (10 cm × 20 cm) are deemed suitable for different standard test methods [104], researchers generally use prismatic and cube samples to measure ECON's electrical resistivity because of sample preparation simplicity.

Resistive heating

In a monotonic heating test, when subjected to a specific voltage for a definite period, ECON experiences a corresponding heat increase. On the other hand, in a cyclic heating method, the sample is subjected to an electrical current for a particular time and then placed at rest for some time, and this procedure is repeated for several cycles to observe the heating and heat-dependent mechanical characteristics of ECON [26]. During melting tests, ice and snow are placed on the ECON samples to observe the ECON deicing performance in the event of ice and snow accumulation on the pavement surface. Resistive heating performance without applying ice and snow on the ECON samples is also done to test ECON performance in preventing any accumulation of ice and snow [55].

Application of advanced concrete technology in ECON

Type I, Type II, and Type V cement dominate in the production of ECON. In addition to conventional concrete, studies on the utilization of Ultra-High-Performance Concrete (UHPC), Light Weight Concrete (LWC), and Self-Consolidating Concrete (SCC) are also evident in the literature, as presented in **Table 2-6**.

Table 2-6 Mix design and engineering properties of UHPC, LWC, and SCC

Items	UHPC [9]	LWC [12]	SCC [40]
ECFs	CFs (Recycled) 0.2 to 0.8 vol.%	CB-0.83 vol.%+ CFs-0.49 vol.%	CFs 0.5 to 0.75 wt.%
Water/binder ratio	0.13	0.41	0.38 to 0.4
Supplementary cementitious materials	Not Available	Fly ash- 21 wt.%	-
Fine Aggregate/cement ratio	1.45	1.40	1.88 to 1.94
Coarse Aggregate/cement ratio	Not Available	Not Available	1.78 to 1.82
Lightweight aggregate/cement ratio	Not Available	1.09	Not Available
Limestone filler/c	0.275	Not Available	Not Available
Sand ratio (vol.%)	Not Available	39	Not Available
Dispersant/cement ratio (wt.%)	Not Available	0.2	Not Available
Superplasticizer (wt.%)	3.75	1.26	0.6 to 0.66
Nano-silica suspension (wt.%)	7.125	Not Available	Not Available
Mixing method	Wet	Wet	Dry
Electrical resistivity (Ω -cm)	60 to 300	63.2	Below 50,000
σ_c (MPa)	80	33.8	Not Available
σ_f (MPa)	16	More than 5	Not Available

A comparative study on conventional concrete and Ultra-High-Performance Concrete (UHPC) revealed that UHPC offers better fiber dispersion, workability, improved mechanical properties, and lower electrical resistivity [39]. Since voids obstruct conductive paths in the ECON matrix, achieving negligible capillary pores in UHPC facilitates improved electrical conductivity [108]. In addition, simplified construction techniques, speedy construction, reduced maintenance, improved durability, improved resiliency, reduced element size and complexity,

minimum interruption of traffic, and extended usage life are other benefits of using UHPC in constructing ECON HPS [109,110].

On the other hand, the low density of LWC makes it easier to heat than conventional ECON [42]. SCC mixes with conductive filler provide lower activation energy values and stable electrical resistivity that justify their application in ECON HPS. Avoiding dispersion difficulty problems associated with ECON is made possible by incorporating SCC technology [111]. Table 6 compares the mix proportioning and engineering properties of UHPC, LWC, and SCC found in different studies.

Full-scale implementation of ECON

ECON's immense potential and success in laboratory study can ease the path to its full-scale implementation. Up to now, ECON HPS has been implemented in the airport apron area (Des Moines International Airport, USA), the entrance lane of a transportation authority (Iowa Department of Transportation, USA), the ramp of a parking space (Harbin, China), road (China), and bridge deck overlay (Roca spur bridge, USA and Bridge 17-75R, Castle Peak, California). Those field-scale projects require in-depth investigation before widespread implementation of ECON HPS can occur.

Key components

Key ECON components are the same for both ordinary pavement and bridge-deck overlay. ECON HPS requires a conductive pavement layer as the heating element, and an ECON heated bridge deck requires a conductive layer over a conventional concrete deck. Electrodes are necessary to convey electricity to the conductive paving material from the power supply. A secure power source ensures a continuous power supply to operate the heated pavement/bridge deck during operation. Temperature sensors are used in heated pavement technology to measure the ambient and the pavement temperature at various locations. A central control system controls

the operation. Surveillance cameras, electrical wiring, polyvinyl chloride conduits, and electrical insulation materials are also vital components of ECON HPS [8,34].

System design

Mandatory steps in designing ECON HPS include determining the required layered thickness for structural adequacy, the electrode configuration, and the estimation of power demand to ensure adequate heating during heated pavement service life [8,34]. To efficiently heat only the surface where ice and snow accumulate, the ECON layer must be placed only on the top portion of the system. Three construction techniques are available for ECON HPS: precast concrete, concrete overlay, and two-lift wet-on-wet paving. Although the use of precast concrete ensures better quality control and rapid construction, the associated cost is high due to transportation placement costs, and the concrete overlay technique is a more cost-effective method, although the lack of data to support long-term performance, overestimating existing pavement thicknesses, and the challenge of having uniform material properties between the existing slab and the ECON slab limit its use [13]. Two-lift wet-on-wet concrete paving technology, constructing a thin ECON layer over a newly-constructed concrete layer reduces the ECON layer thickness and significantly decreases overall construction material costs [8,34], but this technology is practically difficult to implement.

The ECON layer should have a minimum thickness of 76 to 102 mm to avoid any curling or warping-related issues and provide sufficient coverage for the electrodes [23,113]. A 12 m or less joint spacing will secure ECON-heated pavement against longitudinal and transverse cracks, while pressure relief joints are required at a spacing between 300 to 450 m [23]. Since the electrical resistance value increases with the increasing area (A) to length (L), ECON size and geometry influence the electrical properties ratio [46,114]. The heating rate of the ECON slab is

inversely proportional to the cross-sectional area of the slab along the electrodes [23]. **Table 2-7** describes ECON slab sizes and configurations in full-scale field demonstration projects.

Abdullah et al. reported an iterative design flowchart considering the available power source and heat requirements for ECON HPS [15], and a simplified version of the flowchart is presented in **Figure 2-2**, where L , W , and T are the ECON slab's length, width, and thickness. L_s is the distance between the electrodes, and d is between the ECON slab edge and the embedded electrode. R is the electrical resistance, and ρ is the electrical resistivity of the ECON slab. A is the cross-sectional area of the ECON slab parallel to the electrodes. V is the voltage applied to the ECON slab, and I is the current passing through that slab. P_d is the required power density to melt ice and snow accumulated on the ECON slab.

Table 2-7 ECON layer configuration of full-scale HPS

Items	DSM international airport [41]	Harbin parking ramp [42]	Iowa DOT parking lot [43]	Roca Spur bridge [44]
Type of construction	Two-lift construction over 100 mm thick conventional concrete layer	Overlay over an existing slab	Two-lift construction over 178 mm thick conventional Concrete layer	ECON deck over 256 mm conventional RCC deck
Panel size	4.6 m × 3.8 m	2.5 m × 5.6 m	4.6 m × 3.6 m	1.2 m × 4.1 m
ECON thickness	90 mm	90 mm	76 mm	102 mm

However, this system design is only valid for an ECON slab with two electrodes, and since, in field applications, there may be more than two, this system design should be used with caution. In addition, there is no reliability level mentioned in the design process. Hence, this

design process cannot differentiate between ECON for critical infrastructures like airport runways and sidewalks. Required ECON slab size, number of electrodes, and spacing between the electrodes should be chosen if a nearby available power source exists. Otherwise, a transformer may be required to change the voltage level to suit the desired voltage requirement of the system, possibly incurring extra cost and complexity [18].

The system design of the Roca Spur bridge deck was based on the breakdown voltage, the critical voltage threshold above which current will go through the conductive bridge deck as if it were a short circuit. The breakdown voltage value depends on the cross-sectional area, electrode spacing, and material moisture content. In this project, the electrical resistivity of the ECON bridge deck for a given mix design was determined, and then electrode spacing in the ECON slab was determined for a given breakdown voltage [23]. Since the heating rate is proportional to the amount of current flow through ECON, the required current level was determined, and based on this required current, the dimensions of the ECON bridge deck (length, width, and thickness) were determined.

ECON mix design must address project-and location-specific guidelines when selecting material, mix design of concrete, and mixing procedure [9]. **Table 2-8** depicts the mix proportioning of the ECON examples in full-scale pavement construction.

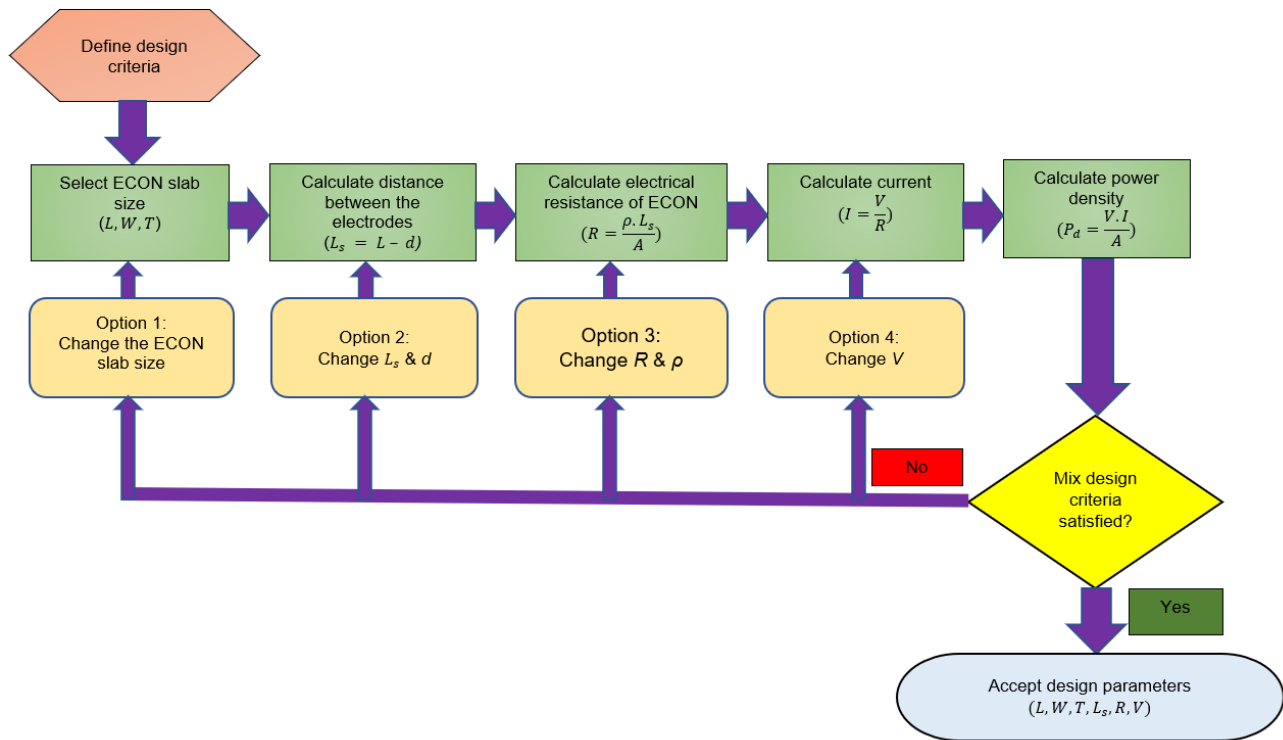


Figure 2-2 Design flow chart for ECON heated slab [6]

ECON mix design and engineering properties

The requirements for the pavement project of Liu et al. were higher workability (>160 mm slump), minimum compressive strength of 30 MPa, lower Modulus of Elasticity (E), and increased flexibility to reduce the noise level during driving, and most importantly, lower resistivity. **Table 2-9** lists the fresh and hardened concrete properties of the ECON developed on this project.

Table 2-8 Mix design of ECON for construction of pavements

Items	DSM international airport [41]	Road in China [45]	Iowa DOT parking lot [43]
ECFs	CFs-1 vol.%	CFs-0.75 vol.%	CFs-1.25 vol.%
Water to cementitious material ratio	0.42	0.65	0.42
Supplementary cementitious materials	Not available	Silica fume-20 wt.%	Fly ash type C-20 wt.%
Fine aggregate/cement (by wt.)	1.42	1.2	1.70
Coarse aggregate/cement (by wt.)	1.25	2.40	1.56
Intermediate aggregate/cement (by wt.)	0.62	Not available	0.80
Sand ratio	0.43	0.33	0.42
Dispersant/cement ratio (wt.%)	0.2	0.7	Not available
Superplasticizer (wt.%)	Not available	2.0	
Mixing Method	Dry	Wet	Dry

Table 2-9 Properties of ECON for road pavement construction

Items	[45]
CFs content	0.75 vol% of concrete
Compressive strength	40 MPa
Splitting tensile strength	2.70 MPa
Slump	163 mm
Electrical resistivity	0.10 Ω -cm

Difficulty in fiber dispersion increases with decreasing fiber diameter. While the dispersion of longer fiber is comparatively more burdensome than for shorter fiber, longer fiber ensures better electrical conductivity [116], and as a result, there is a need to balance to ensure desired electrical performance and workability. The HPS project at the Des Moines International Airport (DSM), Iowa, USA, used CFs (1 vol% of concrete) to produce its ECON layer. 70% of the fibers were of length 6 mm, while the rest were of length 3 mm [8]. An aggregate system

with a CA: IA: FA weight ratio of 38:43:19 was utilized in this project, and a Calcium-Nitrite based corrosion inhibitor (DCI admixture) was utilized to act as a conductivity-enhancing agent. However, since the DCI admixture is an accelerator with its effect becoming more prominent on a hot-sunny casting day, this admixture contributed to poor workability on the placing day.

Table 2-10 Engineering properties of ECON for Airport pavement construction [9]

Items	Sample (Field)	Sample (Laboratory)
Actual CFs content	0.75 vol.% of concrete (0.55 wt.% of cement)	0.98 vol% of concrete (0.74 wt.% of cement)
Compressive strength (MPa)	37	39
Flexural strength (MPa)	7.7	7.6
Air content (%)	7.189	6.004
Slump (mm)	76	38
Electrical resistivity (Ω -cm)	992	115
Void frequency (mm^{-1})	1.678	1.433
Specific surface (mm^{-1})	95.278	96.021
Specific factor (mm)	0.049	0.053
Paste to void ratio	4.968	6.273

According to **Table 2-10**, a discrepancy in the electrical resistivity value between the project's laboratory-prepared and field-prepared samples could be observed despite using identical mix proportioning. In the case of field implementation, researchers attribute such discrepancy to fiber degradation by excessive wear from the aggregates and loss of carbon fibers during mixing [9]. Therefore, an increased amount of conductive filler, CFs at a dosage of 1.25 vol% of concrete, was incorporated into the mix design for ECON of the parking lots of Iowa DOT to ensure optimal CFs dosage. The engineering properties of the produced concrete satisfied the strength criteria for road construction for heavy traffic volume. While incorporating fly ash into the concrete mix increased the workability of this project, it decreased the electrical

conductivity. The reported electrical resistivity of this mixture was 1,300 Ω -cm [34]. The high ECFs content is associated with the dispersion difficulty problem, and securing a uniform dispersion of ECFs is vital for ensuring stable and satisfactory resistive heating performance of ECON HPS at a lower concentration of ECFs.

StF-confined Graphite concrete was used for the parking ramp project in Harbin, China [18]. On the other hand, a hybrid filler comprised of StF (1.5 vol% of concrete) and SSh (20 vol% of concrete) was used for the test bridge deck slab of the Roca spur bridge [4]. **Table 2-11** lists the mix proportioning of the produced ECON, with SSh having a low specific surface area, resulting in more free water in the matrix. The air content of the concrete was also increased by incorporating SSh into the ECON mix, and these factors were responsible for the reduced ECON compressive strength [41].

Table 2-11 Mix design of Test bridge deck for Roca spur Bridge [79]

Items	Content
Cement	14 to 16 vol%
Fine aggregate	10 to 25 vol%
Coarse aggregate	10 to 25 vol%
w/c	0.3 to 0.4

Because of the problems associated with using SSh in the ECON mix, the Roca spur project utilized a hybrid filler of StF (1.5 vol% of concrete) and graphite powder (25 vol% of concrete) to construct the ECON bridge deck. The construction of both the test deck slab and the actual bridge deck followed AASHTO requirements for bridge deck construction, and the workability of the ECON was close to the standard for conventional PCC [117]. **Table 2-12** represents some basic properties of the concrete used in the Roca spur bridge project and the test bridge deck for the Roca spur bridge.

Table 2-12 Properties of ECON for Roca spur bridge deck construction

Items	Test bridge deck of Roca spur bridge [46]	Roca spur bridge deck [47]
Compressive strength (MPa)	31	48
Flexural strength (MPa)	4.6	5.6
Rapid freeze-thaw resistance	No failure after 312 cycles	No failure after 300 cycles
Shrinkage	Less than ACI-209 by 20–30%	Not available
Modulus of elasticity (MPa)	3634	Not available
Permeability(cm ³ /s)	0.004 to 0.007	Not available
Thermal conductivity (W/m- ⁰ K)	10.8	Not available
Unit weight	Not available	2300 kg/m ³
Electrical resistance (Ω -cm)	350 (After 6 months)	300- 500 Ω -cm

Electrodes

Selecting an electrode configuration is one of the vital steps in the ECON HPS design process, and Section 3.5 contains a detailed discussion of electrodes and their effect on ECON performance. In pavement, since the ground layer's temperature remains higher than the ECON slab ambient temperature, pavement ECON will require less power to melt the ice and snow than bridge deck ECON. Consequently, If all the design parameters remain unchanged, the spacing required between the electrodes should be smaller for the bridge deck case than for the pavement [118], and **Table 2-13** lists the electrode configurations used in practical ECON applications. In full-scale ECON HPS construction, stainless steel bar electrodes would be preferred over ordinary steel bars due to their durability and resistance to corrosion [119].

Power supply and operation system

One of the requirements of an ECON HPS system is the power supply to drive the entire system [120], with the utilization of solar or wind energy a possibly viable alternative [90,98]. Although alternating current (AC) resistance is slightly higher than direct current (DC) resistance, heating with an AC power source facilitates electrons taking discrete paths into the conductive paving material to ensure uniform heating in the slab [15,38]. AC power is also more energy-efficient than DC power for a given ECON slab temperature increase [21], and AC ensures a higher heating rate than DC for the same power input [38]. This is why all the full-scale implementations of heated pavements have utilized AC power supplies, as shown in **Table 2-13**.

During a heavy winter storm, air temperature decreases and wind speed increases; consequently, the surface convection coefficient increases, and an increased surface convection coefficient results in an increase in the deicing response time of ECON HPS, and a higher heating rate is required from the ECON to keep the HPS operation time acceptable [121]. Since both the ECON temperature increase rate and power density increase with increased applied voltage [30], an adjustable transformer is desirable for varying the ECON HPS operation to satisfy a variety of snow/ice melting speeds [25].

A control system turns on the ECON HPS system when a snow/ice event begins and off when the system has fully melted the accumulated precipitation. Since preventing snow/ice accumulation is economically more efficient than snow/ice melting after the snow event since less operation time is required in the former case [55,117], turning on the system when the ambient temperature falls below a predetermined point prior to the snow/ice event would be justified. An upper limit for slab temperature should also be set to allow the system to be turned off to prevent system overheating [8,34,117]. Installed temperature sensors are key components

that enable monitoring of the ambient and slab surface temperature, and a central control system manages the process of heating the ECON slab when required. **Table 2-13** lists the characteristics of the control systems used in the full-scale filed ECON HPS projects. A current-monitoring unit can be used to limit the current level in the ECON, and an operator-interface unit helps the user collect temperature and electrical current readings from the ECON slabs.

Table 2-13 Electrode configuration, Power supply, and operation system utilized in full-scale ECON HPS

Items	DSM international airport [41]	Harbin parking ramp [42]	Iowa DOT parking lot [43]	Roca Spur bridge [47]	Bridge 17-75R [48]
Material	Perforated stainless steel	Iron	Stainless steel	Iron	Steel
Size	3.81 cm × 3.81 cm × 0.32 cm	4 cm × 2.5 cm × 0.35 cm	1.9 and 2.5 cm	8.9 cm × 8.9 cm × 0.6 cm	No. 4 rebar
Shape	Angle	Angle	Flat, circular solid, and circular hollow	Angle	Circular
Spacing (cm)	91.46	18	508, 648, and 914	106.7	300
Power supply	AC	AC	AC	AC	Not available
Voltage (V)	240	48	120/208	220	Not available
Operation system	Arduino	Not available	Programmer Logic Controller (PLC)	Microcontroller	Not available

Construction

Since ECON heated-pavement construction includes civil engineering construction, electrical element installation, and control system development, synchronization among all construction divisions is essential for avoiding conflicts that may delay the entire project [120]. ECON heated pavement construction steps can be arranged sequentially, like **Figure 2-3** [6]. Proper bonding must be achieved between the existing pavement layer and the new ECON layer in an overlay construction. The degree of bonding between the existing pavement and ECON layers can be classified as bonded or unbonded [23]. Since even after careful installation during construction, electrical wires connected to electrodes can become disconnected, non-destructive evaluation technology using a magnetic field meter can troubleshoot such disconnected wires [18]. Each gap or excavation in the ECON layer must be filled with high-strength, non-shrink grout mixed with the same ECFs used to produce conductive materials [18]. Drying shrinkage, plastic shrinkage, and traffic loading stress the pavement. Improper ECON curing methods can lead to shrinkage cracking [90]. Thermal stresses developed in the ECON slab depend on thermal strain due to the temperature increase and elastic modulus of concrete [23]. Using a white-pigmented concrete compound can prevent cracking due to drying shrinkage, plastic shrinkage, and thermal stress [8]. In order to prevent electric shock hazards due to stray current at the saw cut line, the Roca Spur bridge project ensured that all the electrodes along the saw cut were at the same voltage [25]. A sawdust mortar thermal insulation layer between the ECON overlay and the concrete bridge deck provides better heat insulation than an epoxy coating or mortar [23].

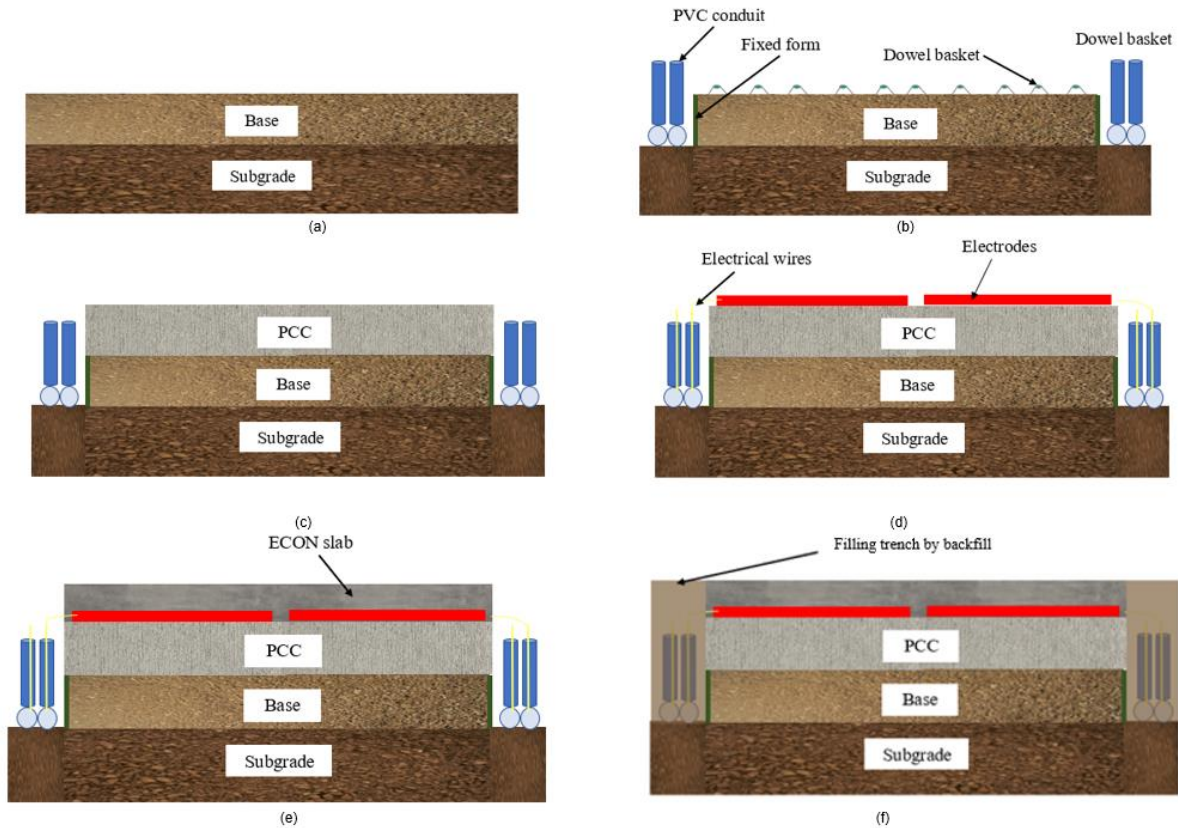


Figure 2-3 Construction steps of ECON HPS: (a) preparation of subgrade and base layer, (b) cutting of trench for placing PVC conduits and placement of dowel baskets, (c) construction of PCC layer, (d) placement of electrodes and wire connections, (e) constructing ECON layer, and (f) backfilling the trench [6]

Performances and costs

The construction and operational costs of an ECON HPS are among the main challenges for large-scale installations.

While the DSM airport project required \$450/m² to construct 10 cm standard concrete and 9 cm ECON concrete, a 19 cm standard concrete slab would be possible at two-thirds of this cost [6]. Constructing the ECON slab layer consumed a significant share of the project cost, as shown in **Figure 2-4**. This ECON system performed well for both anti-icing and deicing cases, even at an ambient temperature of -23.9⁰ C, and about 355 to 419 W/m² [18] of power was

consumed through six winter storms [8]. The ECON layer of the parking ramp project at the Iowa DOT consumed 265.1 W/m^2 power on average to maintain a temperature rise of approximately $0.042^\circ\text{C}/\text{min}$ [34]. The operational cost varies with the ambient temperature, the ice thickness, and the wind speed, with ECON requiring more deicing time for the same power input and consuming more energy for lower ambient temperatures [47]. Since the higher the ambient temperature, the higher the maximum temperature increase [70], a particular site's average winter ambient temperature must be carefully analyzed before designing an ECON-based HPS. Higher power input corresponds to lower electrical resistivity of the conductive paving material [55]. ECON requires less deicing time at higher power input for the same ambient sub-zero temperature and ice thickness. Doubling the ice thickness does not significantly affect the power consumption for the same ambient temperature, meaning that raising the ambient sub-zero temperature to the melting point of snow/ice consumes most of the electric power [47]. The parking ramp project in Harbin, China, required \$1.89 (cost does not reflect inflation) for melting each cubic meter of snow [18].

The construction cost of the ECON deck slab of the Roca spur bridge was $\$635/\text{m}^2$ (the cost does not include the current rate). Purchasing ECFs takes the bulk share of the construction cost, as shown in **Figure 2-5**. The performance of the bridge deck was observed over five years and fourteen winter storms. During the four wind storms, wind speed and ambient temperature varied from 17.9 km/h to 39.9 km/h and -11.7° C to 0.3° C , respectively. The system successfully melted 83.8 mm to 256.5 mm ice thicknesses, consuming 203 W/m^2 to 431 W/m^2 power at an average heating rate $0.14^\circ \text{ C}/\text{min}$. The operational cost of the Roca spur bridge was $\$0.08/\text{m}^2/\text{storm}$ (the cost does not include the current rate) [25].

Operational cost is not prohibitive compared with currently-available alternatives. For example, the deicing cost of one cubic meter of ice without considering the operation and maintenance cost would require \$17.38 and \$15.30 (cost does not reflect inflation) of respective NaCl and MgCl₂ application, while ECON HPS costs only \$1.89 to melt the same amount of ice [18]. In addition, some transportation and city authorities are penalized due to incidents and accidents related to slipping and falling. These factors justify the cost-effectiveness of ECON-based HPS and should be considered among the life cycle costs of ECON HPS. A cost analysis on the application of HPS in airport runway and apron construction reveals a 90% relative likelihood that the benefit-cost ratio would be greater than one [6].

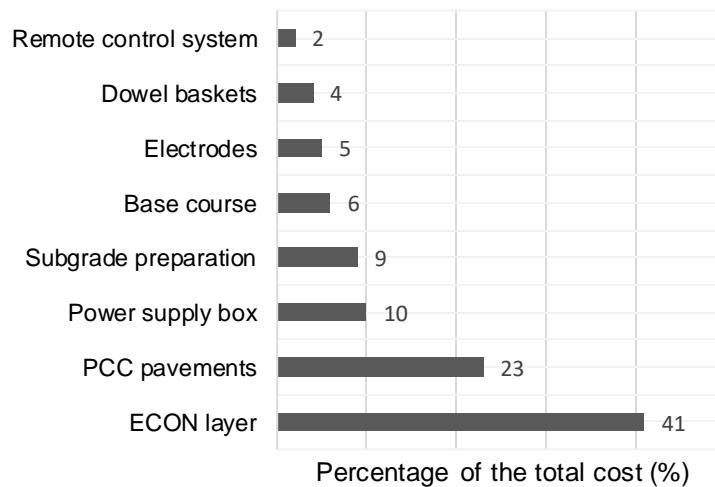


Figure 2-4 Cost breakdown of ECON HPS project in DSM international airport [49]

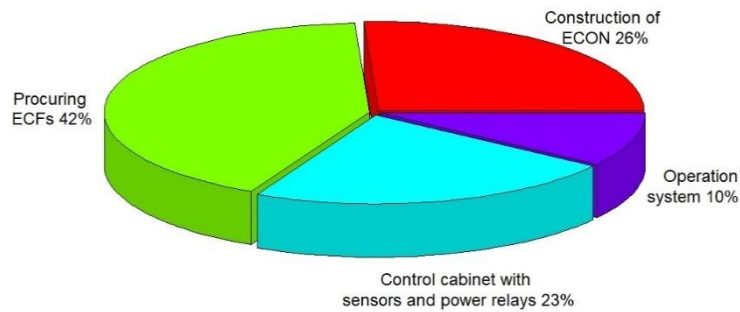


Figure 2-5 Cost breakdown of ECON deck slab Roca spur Bridge Project [50]

Application of ECON resistive heating technology in other civil engineering fields

Indoor radiant heating

Occupant comfort in buildings with low-energy demands can be made possible by utilizing ECON indoor heating floor tiles and partition walls [122]. Hot-water floor radiant systems, electrothermal membrane radiant systems, and heating-cable floor radiant systems are currently available for radiant indoor heating systems [123]. ECON resistive heating technology can be utilized to develop an indoor radiant floor heating system as a viable alternative [122].

An investigation on a laboratory-scale room with a floor size $1.2 \text{ m} \times 0.96 \text{ m}$ and height of 2.0 m , with a window but no furniture, utilized a 20-mm thick radiant floor heating ECON tiles over an RCC floor system, as shown in **Figure 2-6**. **Table 2-14** lists the mix proportioning and the engineering properties of the ECON tiles. The temperature of the center of the room was significantly increased by providing a 32 W/m^2 power input. Self-adhesive PVC floor leather exhibited more heat transfer efficiency than ceramic tiles, and incorporating a reflective film layer prevented heat dissipation into the bottom layer [105].

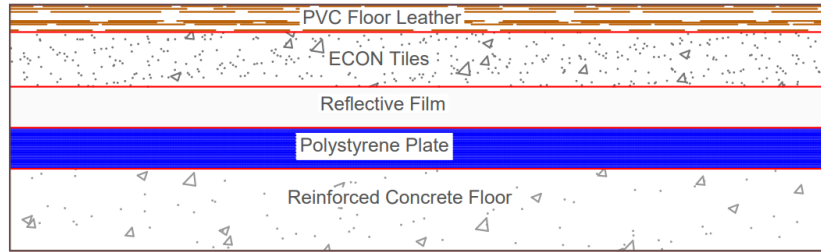


Figure 2-6 Radiant indoor heating ECON layer structure [51]

In another study, 3.5 wt.% CB-doped ECON slabs consumed 123.8 W/m² power to raise the temperature by 100⁰ C within 330 min in a 2.6 m high room with a 1.9 m × 1.8 m floor size. The uniform temperature distribution was observed along the room's height, with indoor air consuming almost half the heat increase. A 70 mm thick white-colored steel panel was sandwiched with expanded polystyrene foam plastic to build the room. The mortar slab's compressive strength, flexural strength, and electrical resistivity were 45 MPa, 7 MPa, and 102 Ω-cm, respectively [123].

Table 2-14 Mix design and engineering properties of ECON used in radiant indoor heating [105]

Items	Details
ECFs	Graphite & StF
Graphite/cement	0.44
Steel fiber/cement	0.18
Fine aggregate/cement	1.92
Coarse aggregate/cement	3.35
Mixing method	Dry
Compressive strength (MPa)	51.60
Electrical resistivity (Ω-cm)	13,297
Heat conductivity co-efficient (W/m-K)	5.60

Since hydration products and internal structures of ionically-conductive mortar blocks have remained unaffected and maintained stable electrical conductivity under repetitive heating conditions, mortar blocks soaked in electrolyte solutions like FeSO₄ or CuSO₄ can be utilized in

radiant indoor heating floor tiles and non-load-bearing partition walls. However, using ionically - conductive mortar in load-bearing walls may cause steel reinforcing bars galvanic corrosion. Therefore, epoxy-coated reinforcing bars or glass fiber-reinforced polymer rebar must be used to construct load-bearing walls if the ionically-conductive mortar is utilized [122].

Ohmic heat curing of concrete

Construction work with concrete in cold regions is susceptible to early frost damage [124–126]. The heaving failures of the free water can affect concrete's mechanical properties and structural performance in low temperatures at an early stage immediately after placement [126–128]. Moreover, repair and reinforcement of concrete structures at ultra-low temperatures require rapid strength formation since, at sub-zero temperatures, cement hydration slowdown significantly [77], and a frost-resisting critical strength of 3.5 MPa should be ensured for concrete construction [73]. Even at normal temperatures, concrete construction requires rapid hydration and corresponding early strength gain to reduce the construction period interval [68], and resistive-heating curing may be a practical solution in such situations. Resistive heating can produce adequate heat for curing concrete, with the method for using resistive heating called ohmic heat curing [126]. Ohmic heat curing can be an alternative to warm shed and thermal storage insulation methods for curing concrete in sub-zero temperature environments [77]

Table 2-15 Mix design and engineering properties of electrically conductive cementitious composites used in ohmic heating

ECFs type and concentration	Mix proportioning	Mechanical properties & Workability	Electrical resistivity (Ω-cm)	Heating performance (TI) ($^{\circ}$ C/min)	References
CNTs 0.6 wt.%	w/c = 0.28 SiF = 10 wt.% SP = 2 wt.%	Slump = 110 ± 5 mm	543.72	0.113	[52]
CFs-0.75 vol.% + CNFs-0.20 vol.%	w/cm = 0.3 FA/c = 1	$\sigma_c = 35.3$ MPa-at 24 h $\sigma_f = 11$ MPa-at 24 h	13.70	0.260	[53]
CFs-0.75 vol.% + CNFs-0.20 vol.%	w/cm = 0.3 FA/c = 1 SP = 2 wt.% Dry Mixing	Not available	17.90	0.328	[33]
CNFs 2.0 vol.%	w/cm = 0.35 FA/c = 1 SP = 1 wt.% Dry Mixing	$\sigma_c = 27.7$ MPa-at 12 h $\sigma_f =$ Approximately 6.25 MPa-at 12 h	36.30	0.203	[54]
GNP 2.0 vol.%	w/cm = 0.35 FA/c = 1 SP = 1.41 vol.% Dry Mixing	$\sigma_c = 24.1$ MPa-at 12 h $\sigma_f =$ Approximately 4 MPa-at 12 h	100.80	0.395	[34]

Liu et al. incorporated 0.2 vol% of CNFs in conjunction with 0.75 vol% CFs into an electrically-conductive mortar sample and obtained a 2-day compressive strength of 49.2 MPa and flexural strength 11.5 MPa after ohmic curing at -20° C. Although the added CNFs did not influence the electrical resistivity of the mortar, a significant improvement in heating performance was observed because of hybridization with CFs. Applying 30 W of constant power that maintained a stable 40-500 C temperature of a mortar sample assisted in cement hydration in extremely low temperatures [77]. During ohmic heating, an increase in electrical resistivity of the cementitious mix occurs due to the heat produced, reducing the moisture level of the pore solution and the concrete hydration [68]. At the same ambient temperature, 2.0 vol% CNFs mortar subjected to a constant voltage of 24 V achieved a compressive strength of 27.7 MPa after 12 h, compared to 0.1 MPa for the sample not subjected to ohmic heating [126]. **Table 2-15** represents some laboratory-scale study data on ohmic heat curing.

If electrical curing is carried out earlier than the mix's 4-6 h age, an increase in porosity and decrease in strength due to differential thermal expansion of the constituent materials can also occur [129]. Kim et al. also observed a reduction in compressive strength if ohmic curing of the mix is started within a six-hour interval. Since incorporating ECFs significantly increases the cost of construction, incorporating ohmic heating in all components of a project may not be cost-effective. Kim et al. embedded small electrically-conductive cementitious material block samples to verify the capability of ohmic heating to accelerate curing and reduce thermal cracks [68]. An ohmic heat curing system design should determine the heat required to cure the entire concrete structure, the amount of electrically-conductive cementitious blocks needed to satisfy the heat requirement, and the required electrical resistivity of the electrically-conductive cementitious blocks to supply enough heat for the ohmic heating curing process of the bulk structure.

Challenges and future recommendations

ECON HPS technology can make winter maintenance operations automated, sustainable, and environmentally friendly, saving transportation agencies billions of dollars. However, gleaning the full potential from ECON HPS has not been possible. The significant challenges that ECON HPS needs to overcome are as follows:

1) Initial construction cost is a hurdle. In pavement, the ECON layer construction cost was roughly two-fifths of the DSM international Airport HPS project total cost, and the cost of the conductive filler accounted for approximately 42% of the capital needed to construct the ECON deck layer of the Roca spur bridge. Reducing construction costs could be made possible by ensuring high ECON conductivity at a lower concentration of ECFs.

2) Consistency of construction quality of ECON between laboratory and f implementation is a significant issue. In addition, since the existing mixing method of ECON and dispersion techniques of ECFs in ECON have failed to produce more cost-effective ECON in large-scale field implementation, future researchers should address this issue.

3) The aggregate volume is two-thirds of the ECON volume, and ECON's electrical resistivity and heating performance are primarily contingent upon the aggregate system. Future researchers should seek an aggregate system that would create a balance between electrical resistivity and durability of concrete.

4) Since the lack of a proper design code and construction specification inhibits transportation agencies from the widespread implementation of ECON HPS technology, future studies should address this.

5) Since mechanical strength and resistive-heating performance requirements for a pedestrian sidewalk should not be the same as those for an airport runway, a concrete mix design for heavy-traffic volume pavement should differ from a low or medium-traffic volume

pavement. However, almost all existing literature focuses only on producing ECON without specifying its end-use. Future studies should present different ECON mix proportions for different applications.

6) Ensuring stable electrically-conductive performance over the design period is vital because operational cost increases with an increasing electrical resistivity. The effect of pavement deterioration on the performance of ECON-heated pavement is more sensitive than that for regular rigid pavement since even the slightest crack may increase the electrical resistivity of ECON [98]. The pavement-deterioration behavior of ECON heated pavement requires in-depth investigation. Although the literature review suggests that embedded electrodes do not affect bottom-up crack propagation in the pavement structure, studies have been limited to 2D finite-element analysis. Incorporating gear configuration and thermal loading is necessary to understand the effect of electrodes on bottom-up cracking comprehensively, and the top-down cracking behavior of ECON also requires investigation [133].

7) Electrodes must be placed a certain depth below the pavement body to ensure no disturbance in pavement mechanical performance under structural loads [1]. In the case of heat-pipe HPS, the embedded depth of the heated pipes affects the pavement's cooling rate, and a drastic drop in the paving surface temperature may cause cracking [1,132].

8) HPS performance depends on geographical location [1]. ECON materials can serve economically up to a specific temperature level of about -250 C, below which they lose their potential for use as a heating element.

9) Finally, safety concerns associated with ECON HPS impede its mass application. The human body perceives electric shock when conducting an electric current above 1 mA [134]. Since ECON slab surfaces under 208 V reported 15 to 30 mA of current in the Roca spur bridge

project [25], a protective layer would be necessary on any exposed ECON surface layer. So far, epoxy coating and polyethylene film have been used as effective measures to prevent potential stray currents without disturbing the heating performance of ECON [18,25]. The skid-resistance performance of ECON HPS after applying such pavement coating requires further evaluation. Further studies are required to develop ECON without safety-related concerns.

Conclusions

The multifunctional capability of electrically-conductive concrete (ECON) heated pavement systems (HPS) gives them the reputation of innovative materials that the future construction industry can embrace. ECON HPS integrates conductive filler materials (ECFs) into standard concrete, giving resistive heating capability. Under applied electric voltage, ECON generates heat that melts ice and snow accumulated on the pavement. This technology is more efficient and environmentally friendly than other passive and active snow removal techniques. Even with its potential as an economically practical alternative snow and ice removal technique, field implementation of ECON HPS has not been widespread. This study discussed ECON HPS technology both from the perspective of laboratory study and field implementation and successfully attempted to define the challenges to the mass application of this technology. The higher initial construction costs of ECON-heated pavement is often identified as the main challenge that ECON HPS must overcome to ensure its widespread implementation. Further studies are necessary to find cost-effective ECFs since it is the most expensive element in the ECON mix. The availability of a design code and construction specification for ECON HPS would encourage transportation agencies to construct demonstration projects. More ECON HPS demonstration projects and related studies would eliminate the lack of guidance for rehabilitation and safety concerns of ECON-heated pavement. ECON HPS could then become an economical

alternative to conventional snow removal techniques. Further studies could be conducted to overcome the research gaps presented in this study.

Acknowledgments

The authors would like to thank the Iowa Department of Transportation (DOT) and the Iowa Highway Research Board (IHRB) for providing the matching funds for this research study, sponsored by the Federal Aviation Administration (FAA). The authors would also like to thank the FAA Air Transportation Center of Excellence for the Partnership to Enhance General Aviation Safety, Accessibility, and Sustainability (PEGASAS). The authors would also like to express their sincere gratitude to other research team members from the Iowa State University PROSPER at the InTrans for their assistance in this research study. Although the Iowa DOT has sponsored this study, they neither endorse nor reject any comments made in this paper. This paper does not constitute a standard, specification, or regulation.

References

- [1] Z. Chi, T. Yiqiu, C. Fengchen, Y. Qing, X. Huining, Long-term thermal analysis of an airfield-runway snow-melting system utilizing heat-pipe technology, *Energy Convers. Manag.* 186 (2019) 473–486. <https://doi.org/10.1016/j.enconman.2019.03.008>.
- [2] A. Malakooti, H. Abdualla, S. Sadati, H. Ceylan, S. Kim, K. Cetin, Experimental and theoretical characterization of electrodes on electrical and thermal performance of electrically conductive concrete, *Compos. Part B Eng.* 222 (2021) 109003. <https://doi.org/10.1016/j.compositesb.2021.109003>.
- [3] R. Hasan, An evaluation of electrically conductive asphalt mixtures for electrically heated flexible pavement systems, (2021).
- [4] S.A. Yehia, C.Y. Tua, Thin conductive concrete overlay for bridge deck deicing and anti-icing, *Transp. Res. Res.* (2000) 45–53. <https://doi.org/10.3141/1698-07>.
- [5] X. Zha, H. Hu, C. Zhang, T. Luo, Development and Laboratory Simulation Tests of Anti - skidding Ice Melting Cushion with Carbon Fibers for Pavement, *Int. J. Pavement Res. Technol.* (2021). <https://doi.org/10.1007/s42947-021-00086-2>.

- [6] A. Nahvi, S.M.S. Sadati, K. Cetin, H. Ceylan, A. Sassani, S. Kim, Towards resilient infrastructure systems for winter weather events: Integrated stochastic economic evaluation of electrically conductive heated airfield pavements, *Sustain. Cities Soc.* 41 (2018) 195–204. <https://doi.org/10.1016/j.scs.2018.05.014>.
- [7] A. Jamil, S. Riaz, M. Ashraf, M.R. Foolad, Gene expression profiling of plants under salt stress, *CRC. Crit. Rev. Plant Sci.* 30 (2011) 435–458. <https://doi.org/10.1080/07352689.2011.605739>.
- [8] H. Abdualla, H. Ceylan, S. Kim, M. Mina, K.S. Cetin, P.C. Taylor, K. Gopalakrishnan, B. Cetin, S. Yang, A. Vidyadharan, Design and Construction of the World’s First Full-Scale Electrically Conductive Concrete Heated Airport Pavement System at a U.S. Airport, *Transp. Res. Rec.* 2672 (2018) 82–94. <https://doi.org/10.1177/0361198118791624>.
- [9] A. Sassani, H. Ceylan, S. Kim, A. Arabzadeh, P.C. Taylor, K. Gopalakrishnan, Development of Carbon Fiber-modified Electrically Conductive Concrete for Implementation in Des Moines International Airport, *Case Stud. Constr. Mater.* 8 (2018) 277–291. <https://doi.org/10.1016/j.cscm.2018.02.003>.
- [10] Y. Farnam, M. Krafcik, L. Liston, T. Washington, K. Erk, B. Tao, J. Weiss, Evaluating the Use of Phase Change Materials in Concrete Pavement to Melt Ice and Snow, *J. Mater. Civ. Eng.* 28 (2016) 04015161. [https://doi.org/10.1061/\(asce\)mt.1943-5533.0001439](https://doi.org/10.1061/(asce)mt.1943-5533.0001439).
- [11] A. Arabzadeh, H. Ceylan, S. Kim, K. Gopalakrishnan, A. Sassani, Superhydrophobic coatings on asphalt concrete surfaces: Toward smart solutions for winter pavement maintenance, *Transp. Res. Rec.* 2551 (2016) 10–17. <https://doi.org/10.3141/2551-02>.
- [12] H. Ceylan, K. Gopalakrishnan, S. Kim, W. Cord, Heated Transportation Infrastructure Systems: Existing and Emerging Technologies, 12th Int. Symp. Concr. Roads. (2014). https://lib.dr.iastate.edu/cgi/viewcontent.cgi?article=1018&context=ccee_conf.
- [13] H. Abdualla, Design, construction, and performance of heated concrete pavements system, (2018). <https://lib.dr.iastate.edu/etd/16268/>.
- [14] B. Han, S. Ding, X. Yu, Intrinsic self-sensing concrete and structures: A review, *Meas. J. Int. Meas. Confed.* 59 (2015) 110–128. <https://doi.org/10.1016/j.measurement.2014.09.048>.

- [15] H. Abdualla, H. Ceylan, S. Kim, K. Gopalakrishnan, P.C. Taylor, Y. Turkan, System requirements for electrically conductive concrete heated pavements, *Transp. Res. Rec.* 2569 (2016) 70–79. <https://doi.org/10.3141/2569-08>.
- [16] A. Arabzadeh, M.A. Notani, A. Kazemiyan Zadeh, A. Nahvi, A. Sassani, H. Ceylan, Electrically conductive asphalt concrete: An alternative for automating the winter maintenance operations of transportation infrastructure, 2019. <https://doi.org/10.1016/j.compositesb.2019.106985>.
- [17] R. Rao, H. Wang, H. Wang, C.Y. Tuan, M. Ye, Models for estimating the thermal properties of electric heating concrete containing steel fiber and graphite, *Compos. Part B Eng.* 164 (2019) 116–120. <https://doi.org/10.1016/j.compositesb.2018.11.053>.
- [18] R. Rao, J. Fu, Y. Chan, C.Y. Tuan, C. Liu, Steel fiber confined graphite concrete for pavement deicing, *Compos. Part B Eng.* 155 (2018) 187–196. <https://doi.org/10.1016/j.compositesb.2018.08.013>.
- [19] S.M.S. Sadati, K. Cetin, H. Ceylan, A. Sassani, S. Kim, Energy and thermal performance evaluation of an automated snow and ice removal system at airports using numerical modeling and field measurements, *Sustain. Cities Soc.* 43 (2018) 238–250. <https://doi.org/10.1016/j.scs.2018.08.021>.
- [20] H.W. Whittington, J. McCarter, M.C. Forde, The conduction of electricity through concrete, *Mag. Concr. Res.* 33 (1981) 48–60. <https://doi.org/10.1680/mac.1981.33.114.48>.
- [21] S. Yehia, C.Y. Tuan, D. Ferdon, B. Chen, Conductive concrete overlay for bridge deck deicing: Mixture proportioning, optimization, and properties, *ACI Struct. J.* 97 (2000) 172–181. <https://doi.org/10.14359/821>.
- [22] K. Gopalakrishnan, H. Ceylan, S. Kim, S. Yang, H. Abdualla, Electrically conductive mortar characterization for self-heating airfield concrete pavement mix design, *Int. J. Pavement Res. Technol.* 8 (2015) 315–324. [https://doi.org/10.6135/ijprt.org.tw/2015.8\(5\).315](https://doi.org/10.6135/ijprt.org.tw/2015.8(5).315).
- [23] C.Y. Tuan, CONDUCTIVE CONCRETE FOR BRIDGE DECK DEICING AND ANTI-ICING, 1 (2004).
- [24] P. Xie, P. Gu, Y. Fu, J.J. Beaudoin, U.S. Patent 5,447,564, (1995) 1–10.

- [25] C.Y. Tuan, Implementation of conductive concrete for deicing (Roca Bridge) - SPR-P1(04)P565, (2008).
- [26] G.M. Kim, F. Naeem, H.K. Kim, H.K. Lee, Heating and heat-dependent mechanical characteristics of CNT-embedded cementitious composites, *Compos. Struct.* 136 (2016) 162–170. <https://doi.org/10.1016/j.compstruct.2015.10.010>.
- [27] H. Dehghanpour, K. Yilmaz, A more sustainable approach for producing less expensive electrically conductive concrete mixtures: Experimental and FE study, *Cold Reg. Sci. Technol.* 184 (2021) 103231. <https://doi.org/10.1016/j.coldregions.2021.103231>.
- [28] C.Y. Tuan, S. Yehia, Evaluation of electrically conductive concrete containing carbon products for deicing, *ACI Mater. J.* 101 (2004) 287–293. <https://doi.org/10.14359/13362>.
- [29] W. Tian, Y. Liu, B. Qi, W. Wang, Enhanced effect of carbon nanofibers on heating efficiency of conductive cementitious composites under ohmic heating curing, *Cem. Concr. Compos.* 117 (2021) 103904. <https://doi.org/10.1016/j.cemconcomp.2020.103904>.
- [30] J. Wu, J. Liu, F. Yang, Three-phase composite conductive concrete for pavement deicing, *Constr. Build. Mater.* 75 (2015) 129–135. <https://doi.org/10.1016/j.conbuildmat.2014.11.004>.
- [31] M. Hambach, H. Möller, T. Neumann, D. Volkmer, Carbon fibre reinforced cement-based composites as smart floor heating materials, *Compos. Part B Eng.* 90 (2016) 465–470. <https://doi.org/10.1016/j.compositesb.2016.01.043>.
- [32] A. Sassani, A. Arabzadeh, H. Ceylan, S. Kim, S.M.S. Sadati, K. Gopalakrishnan, P.C. Taylor, H. Abdulla, Carbon fiber-based electrically conductive concrete for salt-free deicing of pavements, *J. Clean. Prod.* 203 (2018) 799–809. <https://doi.org/10.1016/j.jclepro.2018.08.315>.
- [33] B. Han, L. Zhang, C. Zhang, Y. Wang, X. Yu, J. Ou, Reinforcement effect and mechanism of carbon fibers to mechanical and electrically conductive properties of cement-based materials, *Constr. Build. Mater.* 125 (2016) 479–489. <https://doi.org/10.1016/j.conbuildmat.2016.08.063>.
- [34] A. Malakooti, W.S. Theh, S.M.S. Sadati, H. Ceylan, S. Kim, M. Mina, K. Cetin, P.C. Taylor, Design and Full-scale Implementation of the Largest Operational Electrically Conductive Concrete Heated Pavement System, *Constr. Build. Mater.* 255 (2020) 119229. <https://doi.org/10.1016/j.conbuildmat.2020.119229>.

- [35] L. Wang, F. Aslani, A review on material design, performance, and practical application of electrically conductive cementitious composites, *Constr. Build. Mater.* 229 (2019) 116892. <https://doi.org/10.1016/j.conbuildmat.2019.116892>.
- [36] D.D.L. Chung, Self-heating structural materials, *Smart Mater. Struct.* 13 (2004) 562–565. <https://doi.org/10.1088/0964-1726/13/3/015>.
- [37] G. Faneca, T. Ikumi, J.M. Torrents, A. Aguado, I. Segura, Conductive concrete made from recycled carbon fibres for self-heating and de-icing applications in urban furniture, *Mater. Constr.* 70 (2020) 1–14. <https://doi.org/10.3989/mc.2020.17019>.
- [38] P. Maleki, B. Iranpour, G. Shafabakhsh, Investigation of de-icing of roads with conductive concrete pavement containing carbon fibre-reinforced polymer (CFRP), *Int. J. Pavement Eng.* 20 (2019) 682–690. <https://doi.org/10.1080/10298436.2017.1326235>.
- [39] G. Faneca, I. Segura, J.M. Torrents, A. Aguado, Development of conductive cementitious materials using recycled carbon fibres, *Cem. Concr. Compos.* 92 (2018) 135–144. <https://doi.org/10.1016/j.cemconcomp.2018.06.009>.
- [40] O. Galao, L. Bañón, F.J. Baeza, J. Carmona, P. Garcés, Highly conductive carbon fiber reinforced concrete for icing prevention and curing, *Materials (Basel)*. 9 (2016). <https://doi.org/10.3390/ma9040281>.
- [41] A.S. El-Dieb, M.A. El-Ghareeb, M.A.H. Abdel-Rahman, E.S.A. Nasr, Multifunctional electrically conductive concrete using different fillers, *J. Build. Eng.* 15 (2018) 61–69. <https://doi.org/10.1016/j.jobe.2017.10.012>.
- [42] M. Sun, Y. Wu, B. Li, X. Zhang, Deicing concrete pavement containing carbon black/carbon fiber conductive lightweight concrete composites, *ICTIS 2011 Multimodal Approach to Sustain. Transp. Syst. Dev. - Information, Technol. Implement. - Proc. 1st Int. Conf. Transp. Inf. Saf.* (2011) 662–668. [https://doi.org/10.1061/41177\(415\)84](https://doi.org/10.1061/41177(415)84).
- [43] H. Dehghanpour, K. Yilmaz, F. Afshari, M. Ipek, Electrically conductive concrete: A laboratory-based investigation and numerical analysis approach, *Constr. Build. Mater.* 260 (2020) 119948. <https://doi.org/10.1016/j.conbuildmat.2020.119948>.
- [44] H. Dehghanpour, K. Yilmaz, Heat behavior of electrically conductive concretes with and without rebar reinforcement, *Medziagotyra*. 26 (2020) 471–476. <https://doi.org/10.5755/j01.ms.26.4.23053>.

- [45] A. Shishegaran, F. Daneshpajoh, H. Taghavizade, S. Mirvalad, Developing conductive concrete containing wire rope and steel powder wastes for route deicing, *Constr. Build. Mater.* 232 (2020) 117184. <https://doi.org/10.1016/j.conbuildmat.2019.117184>.
- [46] T. Wu, R. Huang, M. Chi, T. Weng, A study on electrical and thermal properties of conductive concrete, *Comput. Concr.* 12 (2013) 337–349. <https://doi.org/10.12989/cac.2013.12.3.337>.
- [47] Y.H. Bai, W. Chen, B. Chen, R. Tu, Research on electrically conductive concrete with double-layered stainless steel fibers for pavement deicing, *ACI Mater. J.* 114 (2017) 935–943. <https://doi.org/10.14359/51700993>.
- [48] W. Dong, Y. Huang, B. Lehane, F. Aslani, G. Ma, Mechanical and electrical properties of concrete incorporating an iron-particle contained nano-graphite by-product, *Constr. Build. Mater.* 270 (2021) 121377. <https://doi.org/10.1016/j.conbuildmat.2020.121377>.
- [49] J. Sun, S. Lin, G. Zhang, Y. Sun, J. Zhang, C. Chen, A.M. Morsy, X. Wang, The effect of graphite and slag on electrical and mechanical properties of electrically conductive cementitious composites, *Constr. Build. Mater.* 281 (2021) 122606. <https://doi.org/10.1016/j.conbuildmat.2021.122606>.
- [50] J. Li, Q. Qin, J. Sun, Y. Ma, Q. Li, Mechanical and conductive performance of electrically conductive cementitious composite using graphite, steel slag, and GGBS, *Struct. Concr.* (2020) 1–15. <https://doi.org/10.1002/suco.202000617>.
- [51] D. Wang, Q. Wang, Z. Huang, Investigation on the poor fluidity of electrically conductive cement-graphite paste: Experiment and simulation, *Mater. Des.* 169 (2019) 107679. <https://doi.org/10.1016/j.matdes.2019.107679>.
- [52] Y. Ding, Z. Chen, Z. Han, Y. Zhang, F. Pacheco-Torgal, Nano-carbon black and carbon fiber as conductive materials for the diagnosing of the damage of concrete beam, *Constr. Build. Mater.* 43 (2013) 233–241. <https://doi.org/10.1016/j.conbuildmat.2013.02.010>.
- [53] W. Zhang, J. Ouyang, Y. Ruan, Q. Zheng, J. Wang, X. Yu, B. Han, Effect of mix proportion and processing method on the mechanical and electrical properties of cementitious composites with nano/fiber fillers, *Mater. Res. Express.* 5 (2018). <https://doi.org/10.1088/2053-1591/aaa60a>.

- [54] X. Cui, B. Han, Q. Zheng, X. Yu, S. Dong, L. Zhang, J. Ou, Mechanical properties and reinforcing mechanisms of cementitious composites with different types of multiwalled carbon nanotubes, *Compos. Part A Appl. Sci. Manuf.* 103 (2017) 131–147.
<https://doi.org/10.1016/j.compositesa.2017.10.001>.
- [55] J. Gomis, O. Galao, V. Gomis, E. Zornoza, P. Garcés, Self-heating and deicing conductive cement. Experimental study and modeling, *Constr. Build. Mater.* 75 (2015) 442–449.
<https://doi.org/10.1016/j.conbuildmat.2014.11.042>.
- [56] A. D’Alessandro, M. Rallini, F. Ubertini, A.L. Materazzi, J.M. Kenny, Investigations on scalable fabrication procedures for self-sensing carbon nanotube cement-matrix composites for SHM applications, *Cem. Concr. Compos.* 65 (2016) 200–213.
<https://doi.org/10.1016/j.cemconcomp.2015.11.001>.
- [57] L. Ahmed Sbia, A. Peyvandi, P. Soroushian, A.M. Balachandra, K. Sobolev, Evaluation of modified-graphite nanomaterials in concrete nanocomposite based on packing density principles, *Constr. Build. Mater.* 76 (2015) 413–422.
<https://doi.org/10.1016/j.conbuildmat.2014.12.019>.
- [58] J. Han, J. Pan, J. Cai, X. Li, A review on carbon-based self-sensing cementitious composites, *Constr. Build. Mater.* 265 (2020) 120764.
<https://doi.org/10.1016/j.conbuildmat.2020.120764>.
- [59] A. D’Alessandro, M. Rallini, F. Ubertini, A.L. Materazzi, J.M. Kenny, Investigations on scalable fabrication procedures for self-sensing carbon nanotube cement-matrix composites for SHM applications, *Cem. Concr. Compos.* 65 (2016) 200–213.
<https://doi.org/10.1016/j.cemconcomp.2015.11.001>.
- [60] A. Meoni, A. D’alessandro, A. Downey, E. García-Macías, M. Rallini, A.L. Materazzi, L. Torre, S. Laflamme, R. Castro-Triguero, F. Ubertini, An experimental study on static and dynamic strain sensitivity of embeddable smart concrete sensors doped with carbon nanotubes for SHM of large structures, *Sensors (Switzerland)*. 18 (2018) 1–19.
<https://doi.org/10.3390/s18030831>.
- [61] F. Naeem, H.K. Lee, H.K. Kim, I.W. Nam, Flexural stress and crack sensing capabilities of MWNT/cement composites, *Compos. Struct.* 175 (2017) 86–100.
<https://doi.org/10.1016/j.compstruct.2017.04.078>.

- [62] F. Azhari, N. Banthia, Cement-based sensors with carbon fibers and carbon nanotubes for piezoresistive sensing, *Cem. Concr. Compos.* 34 (2012) 866–873.
<https://doi.org/10.1016/j.cemconcomp.2012.04.007>.
- [63] A.L. Materazzi, F. Ubertini, A. D’Alessandro, Carbon nanotube cement-based transducers for dynamic sensing of strain, *Cem. Concr. Compos.* 37 (2013) 2–11.
<https://doi.org/10.1016/j.cemconcomp.2012.12.013>.
- [64] D.Y. Yoo, S. Kim, S.H. Lee, Self-sensing capability of ultra-high-performance concrete containing steel fibers and carbon nanotubes under tension, *Sensors Actuators, A Phys.* 276 (2018) 125–136. <https://doi.org/10.1016/j.sna.2018.04.009>.
- [65] M. Abedi, R. Figueiro, A.G. Correia, Ultra-sensitive affordable cementitious composite with high mechanical and microstructural performances by hybrid CNT/GNP, *Materials (Basel)*. 13 (2020). <https://doi.org/10.3390/MA13163484>.
- [66] S.J. Lee, I. You, G. Zi, D.Y. Yoo, Experimental investigation of the piezoresistive properties of cement composites with hybrid carbon fibers and nanotubes, *Sensors (Switzerland)*. 17 (2017). <https://doi.org/10.3390/s17112516>.
- [67] A.L. Pisello, A. D’Alessandro, S. Sambuco, M. Rallini, F. Ubertini, F. Asdrubali, A.L. Materazzi, F. Cotana, Multipurpose experimental characterization of smart nanocomposite cement-based materials for thermal-energy efficiency and strain-sensing capability, *Sol. Energy Mater. Sol. Cells*. 161 (2017) 77–88. <https://doi.org/10.1016/j.solmat.2016.11.030>.
- [68] G.M. Kim, B.J. Yang, G.U. Ryu, H.K. Lee, The electrically conductive carbon nanotube (CNT)/cement composites for accelerated curing and thermal cracking reduction, *Compos. Struct.* 158 (2016) 20–29. <https://doi.org/10.1016/j.compstruct.2016.09.014>.
- [69] Y.C. Choi, Cyclic heating and mechanical properties of CNT reinforced cement composite, *Compos. Struct.* 256 (2021) 113104.
<https://doi.org/10.1016/j.compstruct.2020.113104>.
- [70] H. Lee, S. Park, S. Cho, W. Chung, Correlation analysis of heating performance and electrical energy of multi-walled carbon nanotubes cementitious composites at sub-zero temperatures, *Compos. Struct.* 238 (2020) 111977.
<https://doi.org/10.1016/j.compstruct.2020.111977>.

- [71] S. Jiang, D. Zhou, L. Zhang, J. Ouyang, X. Yu, X. Cui, B. Han, Comparison of compressive strength and electrical resistivity of cementitious composites with different nano- and micro-fillers, *Arch. Civ. Mech. Eng.* 18 (2018) 60–68.
<https://doi.org/10.1016/j.acme.2017.05.010>.
- [72] J. Han, J. Pan, J. Cai, X. Li, A review on carbon-based self-sensing cementitious composites, *Constr. Build. Mater.* 265 (2020) 120764.
<https://doi.org/10.1016/j.conbuildmat.2020.120764>.
- [73] Y. Liu, M. Wang, W. Wang, Electric induced curing of graphene/cement-based composites for structural strength formation in deep-freeze low temperature, *Mater. Des.* 160 (2018) 783–793. <https://doi.org/10.1016/j.matdes.2018.10.008>.
- [74] S. Sun, S. Ding, B. Han, S. Dong, X. Yu, D. Zhou, J. Ou, Multi-layer graphene-engineered cementitious composites with multifunctionality/intelligence, *Compos. Part B Eng.* 129 (2017) 221–232. <https://doi.org/10.1016/j.compositesb.2017.07.063>.
- [75] A. Mohammed, J.G. Sanjayan, W.H. Duan, A. Nazari, Incorporating graphene oxide in cement composites: A study of transport properties, *Constr. Build. Mater.* 84 (2015) 341–347. <https://doi.org/10.1016/j.conbuildmat.2015.01.083>.
- [76] D.D.L. Chung, Electrically conductive cement-based materials, *Adv. Cem. Res.* 16 (2004) 167–176. <https://doi.org/10.1680/adcr.2004.16.4.167>.
- [77] Y. Liu, M. Wang, W. Tian, B. Qi, Z. Lei, W. Wang, Ohmic heating curing of carbon fiber/carbon nanofiber synergistically strengthening cement-based composites as repair/reinforcement materials used in ultra-low temperature environment, *Compos. Part A Appl. Sci. Manuf.* 125 (2019) 105570.
<https://doi.org/10.1016/j.compositesa.2019.105570>.
- [78] E. Yurdakul, Proportioning for performance-based concrete pavement mixtures, PhD. Thesis. (2013) 227.
- [79] S.A. Yehia, CONDUCTIVE CONCRETE OVERLAY FOR BRIDGE DECK DEICING, Dissertation. (1998) 274.
- [80] A. Sassani, H. Ceylan, S. Kim, K. Gopalakrishnan, A. Arabzadeh, P.C. Taylor, Influence of mix design variables on engineering properties of carbon fiber-modified electrically conductive concrete, *Constr. Build. Mater.* 152 (2017) 168–181.
<https://doi.org/10.1016/j.conbuildmat.2017.06.172>.

- [81] Z. Hou, Z. Li, J. Wang, Influence of Aggregates on Properties of Carbon Fiber Electrically Conductive Concrete for Deicing or Snow Melting, in: 2005.
- [82] Z. Hou, Z. Li, J. Wang, Electrical conductivity of the carbon fiber conductive concrete, *J. Wuhan Univ. Technol. Mater. Sci. Ed.* 22 (2007) 346–349.
<https://doi.org/10.1007/s11595-005-2346-x>.
- [83] A. Hamza, D. François, C. Jean-Pierre, A. Sofiane, B. Yves, Carbon-fibred mortar: Effect of sand content and grain size distribution on electrical impedance, *Proc. 2020 Sess. 13th Fib Int. PhD Symp. Civ. Eng.* (2020) 296–303.
- [84] Y. He, L. Lu, S. Jin, S. Hu, Conductive aggregate prepared using graphite and clay and its use in conductive mortar, *Constr. Build. Mater.* 53 (2014) 131–137.
<https://doi.org/10.1016/j.conbuildmat.2013.11.085>.
- [85] B. Chen, B. Li, Y. Gao, T.C. Ling, Z. Lu, Z. Li, Investigation on electrically conductive aggregates produced by incorporating carbon fiber and carbon black, *Constr. Build. Mater.* 144 (2017) 106–114. <https://doi.org/10.1016/j.conbuildmat.2017.03.168>.
- [86] S.R. Armoosh, M. Oltulu, Self-heating of electrically conductive metal-cementitious composites, *J. Intell. Mater. Syst. Struct.* 30 (2019) 2234–2240.
<https://doi.org/10.1177/1045389X19862373>.
- [87] R. Zhao, C.Y. Tuan, D. Fan, A. Xu, B. Luo, Ionically conductive mortar for electrical heating, *ACI Mater. J.* 114 (2017) 923–933. <https://doi.org/10.14359/51700897>.
- [88] K. Zhang, B. Han, X. Yu, Nickel particle based electrical resistance heating cementitious composites, *Cold Reg. Sci. Technol.* 69 (2011) 64–69.
<https://doi.org/10.1016/j.coldregions.2011.07.002>.
- [89] M. Frac, W. Pichór, P. Szoldra, Cement composites with expanded graphite as resistance heating elements, *J. Compos. Mater.* 54 (2020) 3821–3831.
<https://doi.org/10.1177/0021998320921510>.
- [90] E. Heymsfield, A. Osweiler, P. Selvam, M. Kuss, Developing Anti-Icing Airfield Runways Using Conductive Concrete with Renewable Energy, *J. Cold Reg. Eng.* 28 (2014) 04014001. [https://doi.org/10.1061/\(asce\)cr.1943-5495.0000064](https://doi.org/10.1061/(asce)cr.1943-5495.0000064).
- [91] Y. Lai, Y. Liu, D.X. Ma, The influence of preparation method and electrode on properties of carbon fiber electrically conductive concrete, *Appl. Mech. Mater.* 584–586 (2014) 1035–1038. <https://doi.org/10.4028/www.scientific.net/AMM.584-586.1035>.

- [92] W. Chuang, P. Lei, L. Bing-liang, G. Ni, Z. Li-ping, L. Ke-zhi, Influences of molding processes and different dispersants on the dispersion of chopped carbon fibers in cement matrix, *Heliyon*. 4 (2018). <https://doi.org/10.1016/j.heliyon.2018.e00868>.
- [93] M.Y. Mohd Tadza, T.H.H. Tengku Anuar, F. Mat Yahaya, Investigation on Electrically Conductive Aggregates as Grounding Compound Produced by Marconite, *Civ. Environ. Eng. Reports*. 29 (2019) 86–96. <https://doi.org/10.2478/ceer-2019-0026>.
- [94] H. Zhu, H. Zhou, H. Gou, Evaluation of carbon fiber dispersion in cement-based materials using mechanical properties, conductivity, mass variation coefficient, and microstructure, *Constr. Build. Mater.* 266 (2021) 120891. <https://doi.org/10.1016/j.conbuildmat.2020.120891>.
- [95] W. Chuang, J. Geng-sheng, L. Bing-liang, P. Lei, F. Ying, G. Ni, L. Ke-zhi, Dispersion of carbon fibers and conductivity of carbon fiber-reinforced cement-based composites, *Ceram. Int.* 43 (2017) 15122–15132. <https://doi.org/10.1016/j.ceramint.2017.08.041>.
- [96] B. Han, K. Zhang, X. Yu, E. Kwon, J. Ou, Fabrication of Piezoresistive CNT/CNF Cementitious Composites with Superplasticizer as Dispersant, *J. Mater. Civ. Eng.* 24 (2012) 658–665. [https://doi.org/10.1061/\(asce\)mt.1943-5533.0000435](https://doi.org/10.1061/(asce)mt.1943-5533.0000435).
- [97] W. Dong, W. Li, Z. Tao, K. Wang, Piezoresistive properties of cement-based sensors: Review and perspective, *Constr. Build. Mater.* 203 (2019) 146–163. <https://doi.org/10.1016/j.conbuildmat.2019.01.081>.
- [98] E. Heymsfield, A.B. Osweiler, R.P. Selvam, M. Kuss, Feasibility of Anti-Icing Airfield Pavements Using Conductive Concrete and Renewable Solar Energy, *Fed. Aviat. Adm.* (2013) 65.
- [99] G.M. Kim, B.J. Yang, K.J. Cho, E.M. Kim, H.K. Lee, Influences of CNT dispersion and pore characteristics on the electrical performance of cementitious composites, *Compos. Struct.* 164 (2017) 32–42. <https://doi.org/10.1016/j.compstruct.2016.12.049>.
- [100] H.K. Kim, I.W. Nam, H.K. Lee, Enhanced effect of carbon nanotube on mechanical and electrical properties of cement composites by incorporation of silica fume, *Compos. Struct.* 107 (2014) 60–69. <https://doi.org/10.1016/j.compstruct.2013.07.042>.
- [101] A. Malakooti, M. Maguire, R.J. Thomas, Evaluating Electrical Resistivity as a Performance based Test for Utah Bridge Deck Concrete (CAIT-UTC-NC35), *Rutgers Univ. Cent. Adv. Infrastruct. Transp.* (2018) No. CAIT-UTC-NC35.

- [102] S. Bai, L. Jiang, N. Xu, M. Jin, S. Jiang, Enhancement of mechanical and electrical properties of graphene/cement composite due to improved dispersion of graphene by addition of silica fume, *Constr. Build. Mater.* 164 (2018) 433–441.
<https://doi.org/10.1016/j.conbuildmat.2017.12.176>.
- [103] H. Abdualla, H. Ceylan, S. Kim, M. Mina, K. Gopalakrishnan, A. Sassani, P.C. Taylor, And, K.S. Cetin, Configuration of Electrodes for Electrically Conductive Concrete Heated Pavement Systems, in: *Airf. Highw. Pavements 2017*, 2017.
- [104] S.M.S. Sadati, K.S. Cetin, H. Ceylan, S. Kim, Energy-efficient design of a carbon fiber-based self-heating concrete pavement system through finite element analysis, *Clean Technol. Environ. Policy.* 22 (2020) 1145–1155. <https://doi.org/10.1007/s10098-020-01857-4>.
- [105] R. Zhao, C. Tuan, B. Luo, A. Xu, Radiant heating utilizing conductive concrete tiles, *Build. Environ.* 148 (2019) 82–95. <https://doi.org/10.1016/j.buildenv.2018.10.059>.
- [106] J. Xue, X. Wang, Z. Wang, S. Xu, H. Liu, Investigations on influencing factors of resistivity measurement for graphite tailings concrete, *Cem. Concr. Compos.* (2021) 104206. <https://doi.org/10.1016/j.cemconcomp.2021.104206>.
- [107] I. You, S.J. Lee, G. Zi, D. Lim, Influence of carbon fiber incorporation on electrical conductivity of cement composites, *Appl. Sci.* 10 (2020) 1–13.
<https://doi.org/10.3390/app10248993>.
- [108] V.H. Perry, M. Royce, Innovative field-cast uhpc joints for precast bridge decks (side-by-side deck bulb-tees), village of lyons, new york: design, prototyping, testing and construction, in: *3rd FIB International Congress - 2010*, 2010: pp. 1–13.
- [109] V. Perry, D. Corvez, An Innovative Technology for Accelerated Bridges - The Owner-Designer Dilemma, (2016). <https://doi.org/10.21838/uhpc.2016.3>.
- [110] D. Morandaira, E. Miller, C.T. Jahren, Rapid bridge deck joint repair investigation - Phase III, 2018.
- [111] C. Chang, G. Song, D. Gao, Y.L. Mo, Temperature and mixing effects on electrical resistivity of carbon fiber enhanced concrete, *Smart Mater. Struct.* 22 (2013).
<https://doi.org/10.1088/0964-1726/22/3/035021>.

- [112] R.G. Maggenti, R.R. Carter, R. Meline, Development of Conductive Polyester Concrete for Bridge-Deck Cathodic Protection and Ice Control, *Transp. Res. Rec.* 1597 (1997) 61–69. <https://doi.org/10.3141/1597-08>.
- [113] Table of Contents 2019 ASHRAE Handbook—HVAC Applications, (n.d.). <https://www.ashrae.org/technical-resources/ashrae-handbook/table-of-contents-2019-ashrae-handbook-hvac-applications>.
- [114] H. Dehghanpour, K. Yilmaz, Investigation of specimen size, geometry and temperature effects on resistivity of electrically conductive concretes, *Constr. Build. Mater.* 250 (2020) 118864. <https://doi.org/10.1016/j.conbuildmat.2020.118864>.
- [115] S. Liu, Y. Ge, M. Wu, H. Xiao, Y. Kong, Properties and road engineering application of carbon fiber modified-electrically conductive concrete, *Struct. Concr.* 22 (2021) 410–421. <https://doi.org/10.1002/suco.201900510>.
- [116] D.D. Chung, Dispersion of Short Fibers in Cement, *J. Mater. Civ. Eng.* 17 (2005) 379–383. [https://doi.org/10.1061/\(asce\)0899-1561\(2005\)17:4\(379\)](https://doi.org/10.1061/(asce)0899-1561(2005)17:4(379)).
- [117] C.Y. Tuan, Roca Spur Bridge: The Implementation of an Innovative Deicing Technology, *J. Cold Reg. Eng.* 22 (2008) 1–15. [https://doi.org/10.1061/\(asce\)0887-381x\(2008\)22:1\(1\)](https://doi.org/10.1061/(asce)0887-381x(2008)22:1(1)).
- [118] F. Afshari, K. Yilmaz, H. Dehghanpour, Examination of Electrode Intervals in Electrically Conductive Concretes Produced for Airport Runways by FE Method, (2019). <https://www.researchgate.net/publication/337908563>.
- [119] Z. Hou, Z. Li, J. Wang, Electrically conductive concrete for heating using steel bars as electrodes, *J. Wuhan Univ. Technol. Mater. Sci. Ed.* 25 (2010) 523–526. <https://doi.org/10.1007/s11595-010-0035-x>.
- [120] S.M.S. Sadati, A. Malakooti, K.S. Cetin, H. Ceylan, S. Kim, Proposed Improvements to the Construction of Electrically Conductive Concrete Pavement System Based on Lessons Learned, in: *Constr. Res. Congr. 2020 Comput. Appl.*, 2020: pp. 1049–1056. <https://doi.org/10.1061/9780784482865%0Ahttps://trid.trb.org/view/1760497>.
- [121] X. Zhou, Z.J. Yang, C. Chang, G. Song, Numerical Assessment of Electric Roadway Deicing System Utilizing Emerging Carbon Nanofiber Paper, *J. Cold Reg. Eng.* 26 (2012) 1–15. [https://doi.org/10.1061/\(asce\)cr.1943-5495.0000033](https://doi.org/10.1061/(asce)cr.1943-5495.0000033).

- [122] R.H. Zhao, C.Y. Tuan, A. Xu, D.B. Fan, Conductivity of ionically-conductive mortar under repetitive electrical heating, *Constr. Build. Mater.* 173 (2018) 730–739. <https://doi.org/10.1016/j.conbuildmat.2018.04.074>.
- [123] S. Mingqing, M. Xinying, W. Xiaoying, H. Zuofu, L. Zhuoqiu, Experimental studies on the indoor electrical floor heating system with carbon black mortar slabs, *Energy Build.* 40 (2008) 1094–1100. <https://doi.org/10.1016/j.enbuild.2007.10.009>.
- [124] K.T. Koh, C.J. Park, G.S. Ryu, J.J. Park, D.G. Kim, J.H. Lee, An experimental investigation on minimum compressive strength of early age concrete to prevent frost damage for nuclear power plant structures in cold climates, *Nucl. Eng. Technol.* 45 (2013) 393–400. <https://doi.org/10.5516/NET.09.2012.046>.
- [125] J.S. Ryou, Y.S. Lee, Properties of early-stage concrete with setting-accelerating tablet in cold weather, *Mater. Sci. Eng. A.* 532 (2012) 84–90. <https://doi.org/10.1016/j.msea.2011.10.066>.
- [126] Y. Liu, M. Wang, W. Wang, Ohmic heating curing of electrically conductive carbon nanofiber/cement-based composites to avoid frost damage under severely low temperature, *Compos. Part A Appl. Sci. Manuf.* 115 (2018) 236–246. <https://doi.org/10.1016/j.compositesa.2018.10.008>.
- [127] S.W. Tang, Y. Yao, C. Andrade, Z.J. Li, Recent durability studies on concrete structure, *Cem. Concr. Res.* 78 (2015) 143–154. <https://doi.org/10.1016/j.cemconres.2015.05.021>.
- [128] D.J. Corr, P.J.M. Monteiro, J. Bastacky, Observations of ice lens formation and frost heave in young Portland cement paste, *Cem. Concr. Res.* 33 (2003) 1531–1537. [https://doi.org/10.1016/S0008-8846\(03\)00103-0](https://doi.org/10.1016/S0008-8846(03)00103-0).
- [129] I. Heritage, DIRECT ELECTRIC CURING OF MORTAR AND CONCRETE laD Heritage B . EDg (HoDs), M . Se, (2001).
- [130] E. Yurdakul, P.C. Taylor, H. Ceylan, F. Bektas, Effect of Paste-to-Voids Volume Ratio on the Performance of Concrete Mixtures, *J. Mater. Civ. Eng.* 25 (2013) 1840–1851. [https://doi.org/10.1061/\(asce\)mt.1943-5533.0000728](https://doi.org/10.1061/(asce)mt.1943-5533.0000728).
- [131] B. Han, K. Zhang, T. Burnham, E. Kwon, X. Yu, Integration and road tests of a self-sensing CNT concrete pavement system for traffic detection, *Smart Mater. Struct.* 22 (2013). <https://doi.org/10.1088/0964-1726/22/1/015020>.

- [132] J. Wang, Q. Meng, K. Tan, L. Zhang, Y. Zhang, Experimental investigation on the influence of evaporative cooling of permeable pavements on outdoor thermal environment, *Build. Environ.* 140 (2018) 184–193.
<https://doi.org/10.1016/j.buildenv.2018.05.033>.
- [133] S.M.S. Sadati, A. Rezaei-tarahomi, K.S. Cetin, H. Ceylan, Integrated Fracture Mechanics and Finite Element Analysis of an Electrically Conductive Concrete Heated Pavement System, in: 2019: pp. 1–7.
- [134] R. Fish, L. Geddes, Educación Popular en la elaboración de materiales para capacitación en TICs para el desarrollo social, (2009) 407–421.

CHAPTER 3. DEVELOPMENT OF ELECTRICALLY CONDUCTIVE CONCRETE FOR THE CITY OF IOWA CITY SIDEWALK ENHANCEMENT PROJECT

Md Lutfor Rahman¹, Amir Malakooti¹, Halil Ceylan², Peter C. Taylor⁴, Sunghwan Kim⁴

¹Graduate Research Assistant, Department of Civil, Construction and Environmental Engineering (CCEE), Iowa State University, Ames, IA 50011, United States

²Professor of CCEE, ISU Site Director, FAA Partnership to Enhance General Aviation Safety, Accessibility and Sustainability (PEGASAS) Center of Excellence (COE) on General Aviation Director, Program for Sustainable Pavement Engineering and Research (PROSPER), CCEE, Iowa State University, Ames, IA 50011-1066, United States

³Research Professor of CCEE, Director of National Concrete Pavement Technology Center, Ames, IA 50010-8664, United States

⁴Research Scientist, Institute for Transportation, CCEE, Iowa State University, Ames, IA 50011-1066, United States

Modified from a manuscript published in *14th International Symposium on Concrete Roads*

Abstract

Electrically conductive concrete (ECON) heated pavement system is a promising alternative to traditional snow and ice removal procedures that use de-icing chemicals and snow-removal equipment. Using carbon fiber in the ECON mix design, ECON becomes electrically conductive and can produce heat through resistive heating when a voltage is applied. Full-scale field demonstrations of the ECON heated pavement system at the Des Moines International Airport (DSM) and the Iowa Department of Transportation (DOT) central offices reveal the electrical resistivity of ready-mix concrete plant-produced ECON is approximately ten times higher than in the laboratory. Higher ECON electrical resistivity decreases the ECON thermal performance and increases the time required to melt ice and snow. This study aimed to produce ECON with as lower electrical resistivity as possible in the laboratory so that the electrical resistivity remains within the needed values in the field. This study utilizes ACI 211 and the performance-engineered mixture (PEM) design methodology. Ten mixtures were produced in the

laboratory using ACI 211 and PEM techniques. The results suggest that beyond the percolation threshold of carbon fiber in the mixture, the cement paste quantity, aggregate system, and aggregate gradation mainly govern the performance of the ECON. The results of this study will provide a better understanding of developing an optimized ECON mix design that can be used for the future construction of the Iowa City sidewalk ECON heated pavement system project.

Introduction

Transportation agencies actively seek innovative pavement ice and snow removal technologies because snow and ice accumulation on pavement impede traffic operations and decrease safety [1]. In addition, transportation agencies incur enormous costs in materials and labor in snow removal efforts [2]. Agencies currently rely on methods involving chemicals and mechanical methods [3]. However, the chemicals in use now can be harmful to the pavement structure and the environment [4,5]. Mechanical methods are not always effective, depending on the temperatures and traffic loading during the snow event.

Superhydrophobic coatings, resistive cable heated pavements, hydronically-heated pavements, phase-change-materials, and electrically conductive concrete (ECON) heated pavement are innovative snow removal technologies under investigation that utilize minimum human labor and solve the pavement snow and ice issue automatically.

The ECON heated pavement system (HPS) appears promising among the recently developed snow removal methods and has been demonstrated in several global locations in the USA and China.

An electrically conductive concrete layer is the heart of the ECON system. Electrically conductive materials such as carbon fiber, steel fiber, stainless steel shavings, graphene powder, carbon black, and carbon nanotube are widely used in electrically conductive concrete to

increase the electrical conductivity of concrete. When electricity is applied to electrodes embedded inside the concrete, heat is generated through the resistive effects of the material. It is essential to provide a mixture with the correct electrical resistivity. The lower the electrical resistivity, the higher the temperature increase rate and the lower the operation cost [1].

Field-scale production of ECON is challenging because the electrical resistivity of ready-mix concrete plant-produced ECON is generally higher than that of laboratory mixtures. The field electrical resistivity was almost ten times higher than in the laboratory in the DSM and Iowa DOT ECON projects [6,7]. This is likely due to fiber degradation during mixing operation; therefore, this team investigated producing ECON with as low electrical resistivity as possible in the laboratory so that during field production, the value will be below the desirable limit of 1,000 Ω -cm [3].

The coarse, fine, and intermediate aggregate combination can be termed an aggregate system. The aggregate system comprises almost three-quarters of the volume of an ECON mixture. Therefore, any change in the aggregate physical or chemical properties or the aggregate gradation should impact the performance of ECON, but research on this aspect is rare [1]. According to the literature, aggregate systems control the cement paste quantity of the mixture [8]. However, cement paste's effect on ECON's performance has not been investigated so far, although cement paste is the second most electrically conductive material in the phases of ECON.

This study aims to produce ECON with as low electrical resistivity as possible for the Iowa City bus stop enhancement project. Ten mixtures were produced in the laboratory, and their relative performance was evaluated. The outcome of this study will assist in understanding the

importance of cement paste, aggregate gradation, and aggregate system on the performance of ECON.

Materials and Methods

All materials used in this study conformed to the Iowa Statewide Urban Design and Specifications (SUDAS) and the Iowa Department of Transportation (Iowa DOT) specifications for sidewalk construction. Type-I/II Cement complying with ASTM C150 standard with a specific gravity of 3.15 was used in this study. This study's aggregates (coarse, intermediate, and fine) were from two different sources. Properties of the aggregates are presented in Table 3-1. 6-mm long chopped carbon fiber (7.2 μm filament diameter) was added into the concrete mixture as an electrically conductive material (electrical resistivity of $1.55 \times 10^{-3} \Omega\text{-cm}$). Air entraining and high-range water reducers were used to achieve a target 6% air content and desirable workability.

The experimental setup for this study is classified into three sub-divisions: E-1, E-2, and E-3. In the first one, four mixtures were produced using the ACI-211 concrete mixture procedure. The cement paste content was increased from Mix-1 to Mix-4. The aggregate system for E-1 mixtures was 39:18:43 (coarse: intermediate: fine aggregate) based on the system used for the DSM International Airport and Iowa DOT ECON HPS. Table 3-2 presents the mix proportions for the E-1 mixtures. Mix-1 is comparable to the mix proportioning of DSM International Airport and Iowa DOT ECON mixture [6,7,9]. In all the mixtures for this study, the cement content is on the higher side because Carbon Fiber increases the shear stress of the mixture and reduces the workability; therefore, cement paste demand increases for this type of concrete [8]. The volume of the added admixtures in this study depends on the weight of the cement utilized. For instance, Mix-1 added an air-entraining agent at a rate of 1.16 ml for each

Kg of cement used in the mixture. Since the cement weight was 472 Kg/m³, 547.50 ml/m³ air entrainment was added to ensure 6% air content for this mixture type.

Table 3-1 – Properties of the aggregates

Type	Property	Ames	Iowa City
Coarse aggregate	Specific gravity	2.68	2.55
	Water absorption (%)	1.98	2.30
	Mineralogy	Limestone	Limestone
	Nominal Maximum Size of Aggregate	25 mm	19 mm
Intermediate aggregate	Specific gravity	2.68	NA
	Water absorption (%)	1.10	NA
	Mineralogy	Limestone	NA
	Nominal Maximum Size of Aggregate	#8	NA
Fine aggregate	Specific gravity	2.65	2.65
	Water absorption (%)	1.83	0.82
	Type	Natural Sand	Natural Sand
NA = Not Applicable			

Table 3-2 – Mixture proportions of the E-1 mixtures

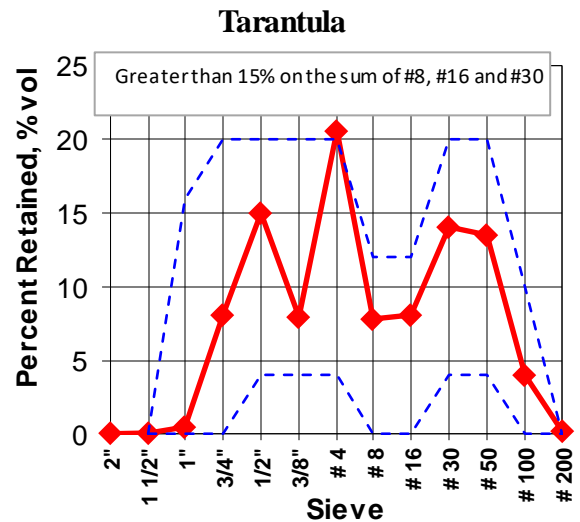
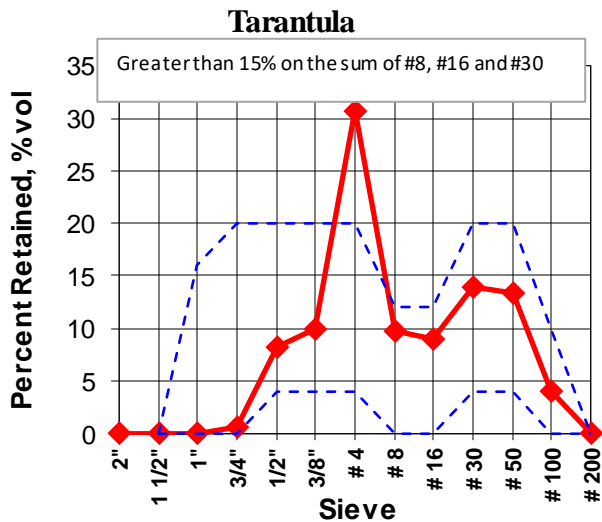
Items	Mix-1 (Kg/m ³)	Mix-2 (Kg/m ³)	Mix-3 (Kg/m ³)	Mix-4 (Kg/m ³)
w/cm	0.42	0.42	0.42	0.42
Cement	472	523	560	592
Coarse aggregate	586	546	519	494
Fine aggregate	651	607	577	549
Intermediate aggregate	296	276	262	249
Water	200	222	237	251
Carbon fiber	28	28	28	28
Air entraining agent (ml/Kg)	1.16	1.16	1.16	1.16
High-range water reducer (ml/Kg)	4.37	4.37	4.37	4.37

However, in the case of five E-2 mixtures in Table 3-3, the performance-engineered mixture (PEM) technique was utilized to develop the mixture proportions [10].

A combination of 45:10:45 (coarse: intermediate: fine) in the aggregate system better fell within the Tarantula curve for materials in hand, as shown in **Figure 3-1**. The addition of carbon fiber increases the shear stress of the mixture, so an increased cement paste to void volume (V_p/V_v) was utilized for all E-2 mixtures [11]. The volume of paste to the V_p/V_v ratios used were 300%, 325%, and 350%, for Mix-5, Mix-6, and Mix-7, respectively. Water-reducer was used for Mixtures 7-WR and 8 to improve workability. Mix-8 had approximately 18% less carbon fiber than other mixtures.

Table 3-3 – Mixture proportions of the E-2 mixtures

Items	Mix-5 (Kg/m ³)	Mix-6 (Kg/m ³)	Mix-7 (Kg/m ³)	Mix-7-WR (Kg/m ³)	Mix-8 (Kg/m ³)
w/cm	0.42	0.42	0.42	0.42	0.42
Cement	483	510	535	535	535
Coarse aggregate	685	662	640	640	643
Fine aggregate	692	669	647	647	649
Intermediate aggregate	137	276	127	127	130
Water	203	132	224	224	224
Carbon fiber	28	28	28	28	23
Air entraining agent (ml/Kg)	1.16	1.16	1.16	1.16	1.16
High-range water reducer (ml/Kg)	-	-	-	4.37	4.37



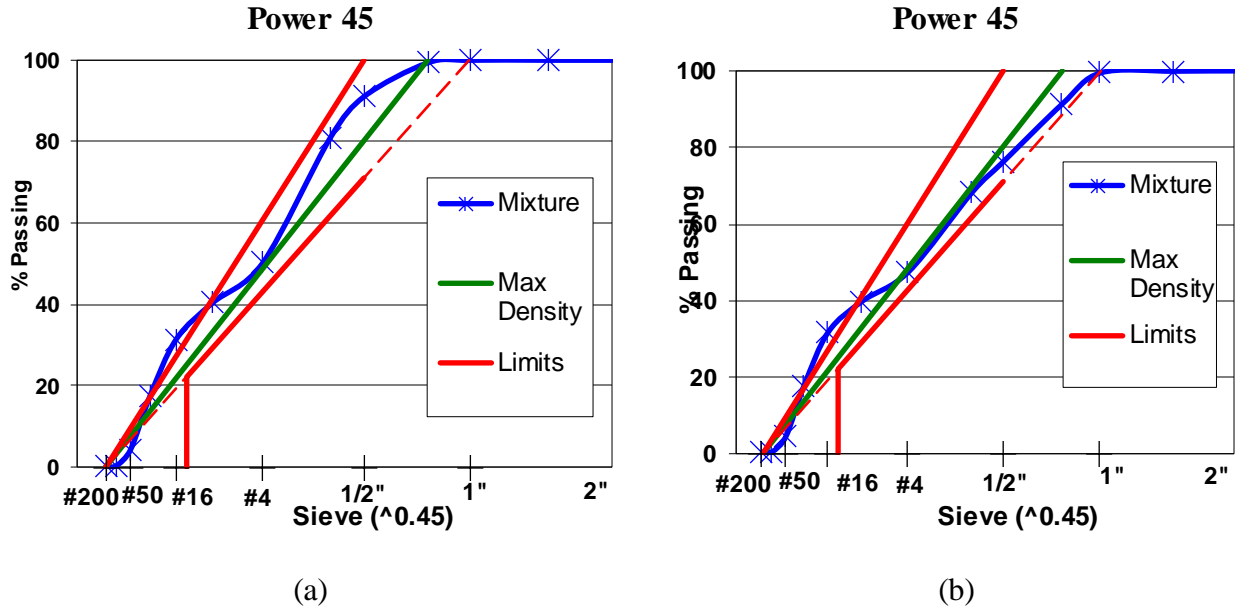


Figure 3-1 Combined aggregate gradation for (a) 45:10:45 aggregate system (b) 38:19:43 aggregate system

Two mixtures designated as Mix-9 and Mix-10 were developed under E-3 using Iowa City aggregates. A 55:45 (coarse: fine) aggregate system for these materials satisfied the Tarantula curve. The cement paste to void volume for Mix-9 and Mix-10 were 350% and 500%, respectively. Table 3-4 provides the mixture proportions of the E-3 mixtures.

Table 3-4 – Mixture proportions of the E-3 mixtures

Items	Mix-9 (Kg/m ³)	Mix-10 (Kg/m ³)
w/cm	0.42	0.42
Cement	417	533
Coarse aggregate	886	764
Fine aggregate	721	621
Water	175	224
Carbon fiber	23	23
Air entraining agent (ml/Kg)	1.02	1.02
Water reducer (ml/Kg)	2.91	2.91

The mixing procedure for all the mixtures in this study followed this sequence:

- All the aggregates were first put into the mixture drum and mixed for 30 seconds.
- Air entraining admixture and 20% of the mixture water were then put into the mixture.
- After mixing the ingredients for 30 seconds, carbon fiber was added and mixed for another 30 seconds.
- The cement and remaining water were then incorporated into the mixture gradually.
- The water-reducing admixtures were added at the very end.

This mixing procedure was found to be suitable for laboratory ECON production. However, field scenarios can be different due to different mixing energy utilized in the ready-mix concrete plant, and it requires further study to minimize the brittle failure of carbon fiber filaments, which is not within the scope of this study.

Workability was measured at the fresh stage for all the mixtures using the VKelly method [5]. If the workability was satisfactory for a particular mixture, $356 \times 100 \times 100$ mm beam samples were prepared for electrical resistivity and thermal performance testing. 100×200 mm cylindrical samples were prepared to evaluate the compressive strength following ASTM C39.

For the beam samples, copper mesh electrodes were installed at the ends for applying voltage from a 120 VAC source. The electrical resistivity was measured using a Southwire true RMS clamp meter, and thermal performance was monitored using a FLIR T650sc infrared thermal camera.

Results and Discussions

E-1 mixtures

The workability and compressive strength of the samples increased as the cement paste content increased from Mix-1 to Mix-4. The V_{kelly} slump was 25 mm for Mix-1 and 50 mm for Mix-4, and the V_{kelly} index was 0.3 and 0.2 cm/\sqrt{s} , respectively, for Mix-1 and Mix-4. A V_{kelly} index in between 2-3 cm/\sqrt{s} is deemed suitable for regular concrete [12]. Since including fiber increases shear stress but still produces workable concrete [6], standardizing the V_{kelly} slump and V_{kelly} index value for fiber-reinforced concrete is necessary.

There was around a 21% increase in the compressive strength of Mix-4 samples compared to the Mix-1 samples because of the higher cement paste content in the former one. In addition to the chemical contribution of using excess cement paste, the increased cement paste assisted in better carbon fiber dispersion, which resulted in the higher compressive strength of Mix-4 samples compared to Mix-1. All the mixtures satisfied the SUDAS specification of 28 MPa for the compressive strength of the concrete at 28 days of curing age.

Mix-2, Mix-3, and Mix-4 had 11%, 19%, and 26% extra paste compared to Mix-1. The aggregate content decreased to accommodate the extra paste for Mix-2 through Mix-4. Since cement paste has lower electrical resistivity than the aggregate used in regular concrete [2], the electrical resistivity of the samples decreased with an increase in the cement paste content, as shown in **Figure 3-2**. However, the rate of decrease in electrical resistivity with increasing cement paste reached a plateau and did not decrease significantly afterward. The increasing cement paste assisted in the fiber dispersion, but after a certain limit, no additional improvement in fiber dispersion occurred, which is why electrical resistivity did not decrease significantly after reaching a plateau.

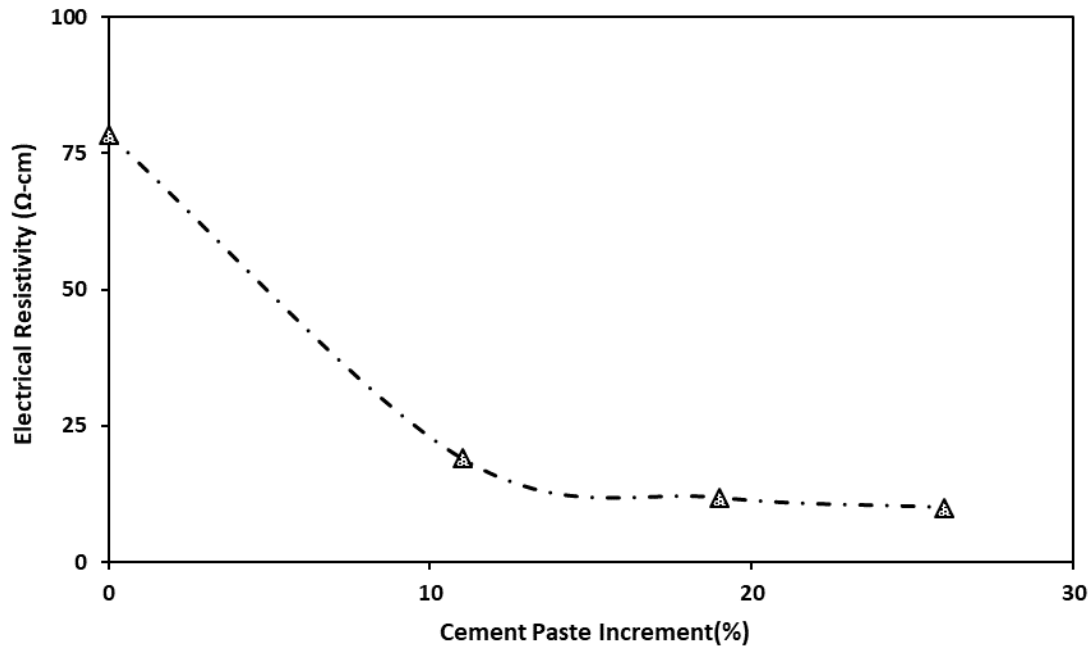


Figure 3-2 Relationship between electrical resistivity and cement paste

According to **Figure 3-3**, the electrical resistivity of ECON samples increases with time, but this increase is not significant enough for samples with lower electrical resistivity (Mix-2 to Mix-4). Since the electrical resistivity measurement of the samples began seven days after curing, it is unknown whether a significant increase in electrical resistivity had already occurred within the first few days of curing; in future studies, electrical resistivity should be observed from the moment of sample casting so that the electrical resistivity increase trend can be better observed. An electrical resistivity prediction model can be developed in such a case, which will assist in evaluating the durability of the ECON HPS.

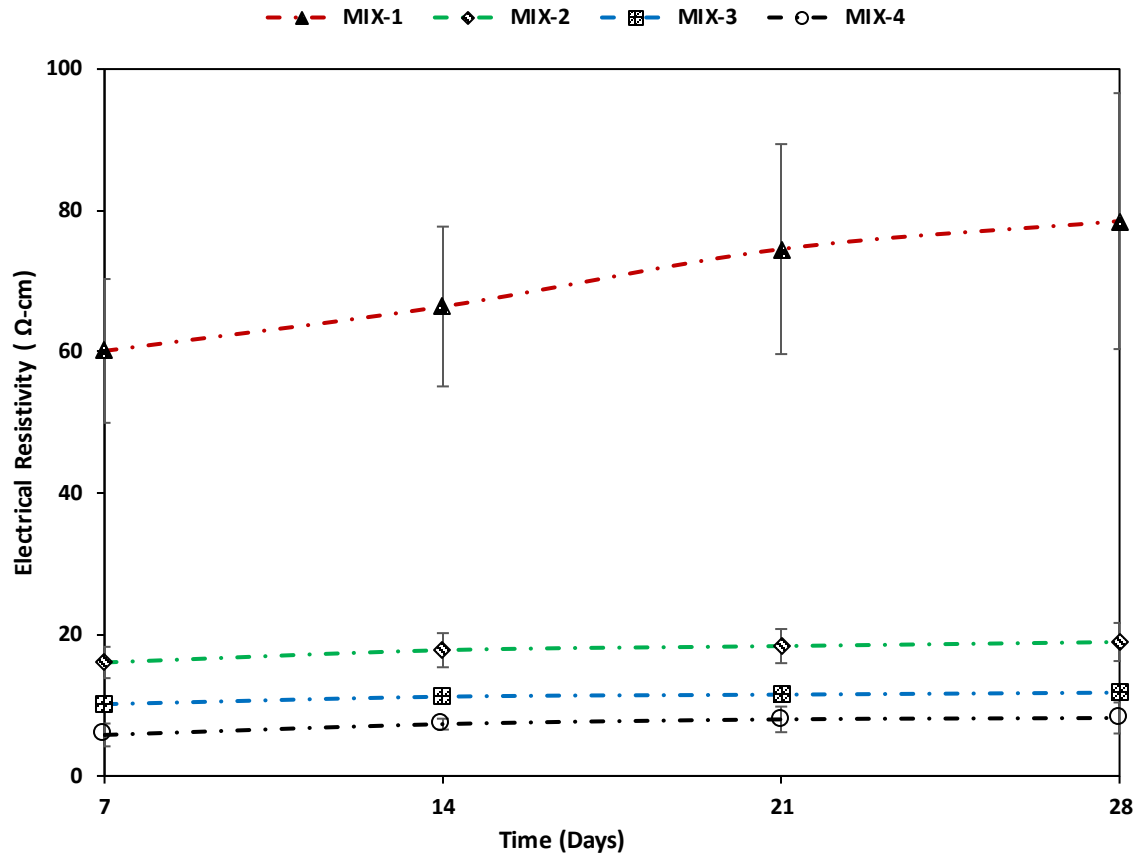


Figure 3-3 Increase in electrical resistivity with time

The thermal performance testing followed a similar trend as the electrical resistivity of the samples; the thermal performance of Mix-4 was better than Mix-1, as shown in **Figure 3-4**. In a hypothetical situation, if the pavement temperature is -100C during a snow event and the system is programmed to operate until the pavement temperature reaches 50C, Mix-1 samples would require 1.5 times more operating time than the Mix-4 samples. As a result, the operation cost will be 1.5 times higher in the case of Mix-1 than in Mix-4.

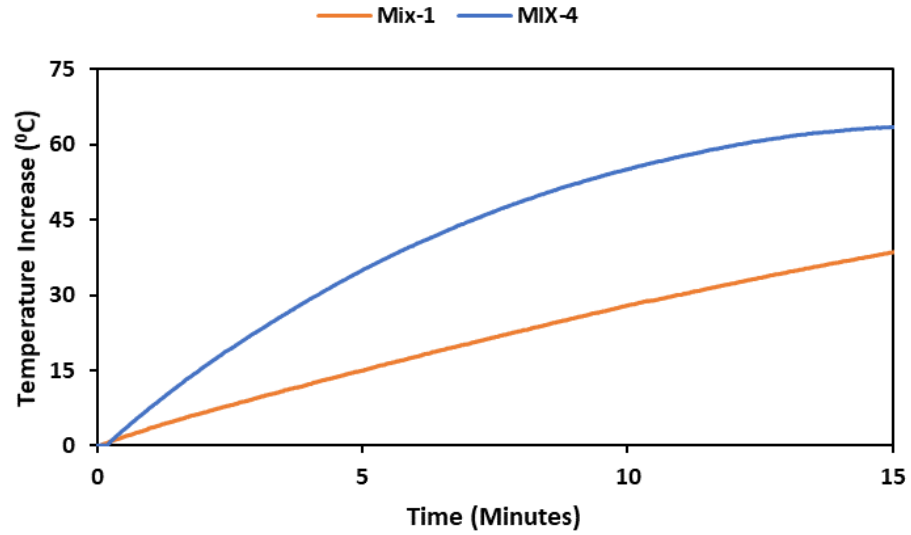
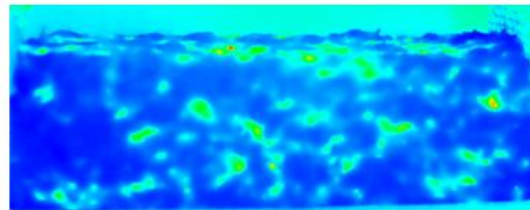
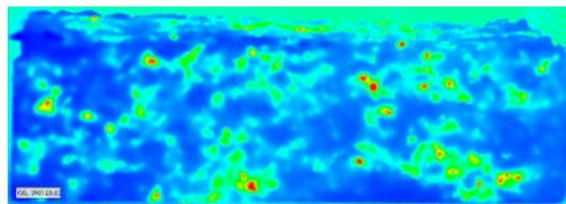


Figure 3-4 Thermal performance of E-1 mixtures

As shown in **Figure 3-5**, the heat was generated from places within the sample where CF was present, and better CF distribution was achieved with an extra amount of paste in the mixtures.



(a)



(b)

Figure 3-5 Distribution of CF within the samples (a) Mix-1 (b) Mix-4

E-2 and E-3 mixtures

E-2 mixtures had more fine aggregate than the E-1 mixtures. Since fine aggregate increases the water requirement for a specific concrete mixture's specific consistency [6], the workability of E-2 mixtures (Mix-5 to Mix-7-WR) went down. There was no measurable V_{kelly} slump for Mix-5 to Mix-7-WR; therefore, no samples were collected from those mixtures. However, workable concrete with a 95 mm V_{kelly} slump was produced from Mix-8, which had 18% less CF than the earlier mixtures. Since carbon fiber's inclusion increases the shear strength of concrete, lowering the dosage rate of carbon fiber in the case of Mix-8 assisted with the workability of ECON compared to Mix-5 to Mix-7-WR. The sample's compressive strength from Mix-8 was 47 MPa. Comparing Mix-4 and Mix-8, the latter utilized less cement paste and carbon fiber than the former. Therefore, it is not always true that increasing cement paste will increase compressive strength.

With a similar $\%V_p/V_v$ to Mix-8, Mix-9 failed to provide any V_{Kelly} slump. As the $\%V_p/V_v$ increased from 350 to 500 for Mix-10, acceptable workability ($V_{K Kelly}$ slump of 55 mm) was achieved, but not to Mix-8. The compressive strength of the Mix-10 sample was 47 MPa, the highest among all the mixtures. Here, it must be noted that the cement paste content of Mix-8 and Mix-10 were almost similar. Therefore, the workability and compressive strength variation between those mixtures are due to the difference in the aggregate source, changed aggregate system, and NMSA.

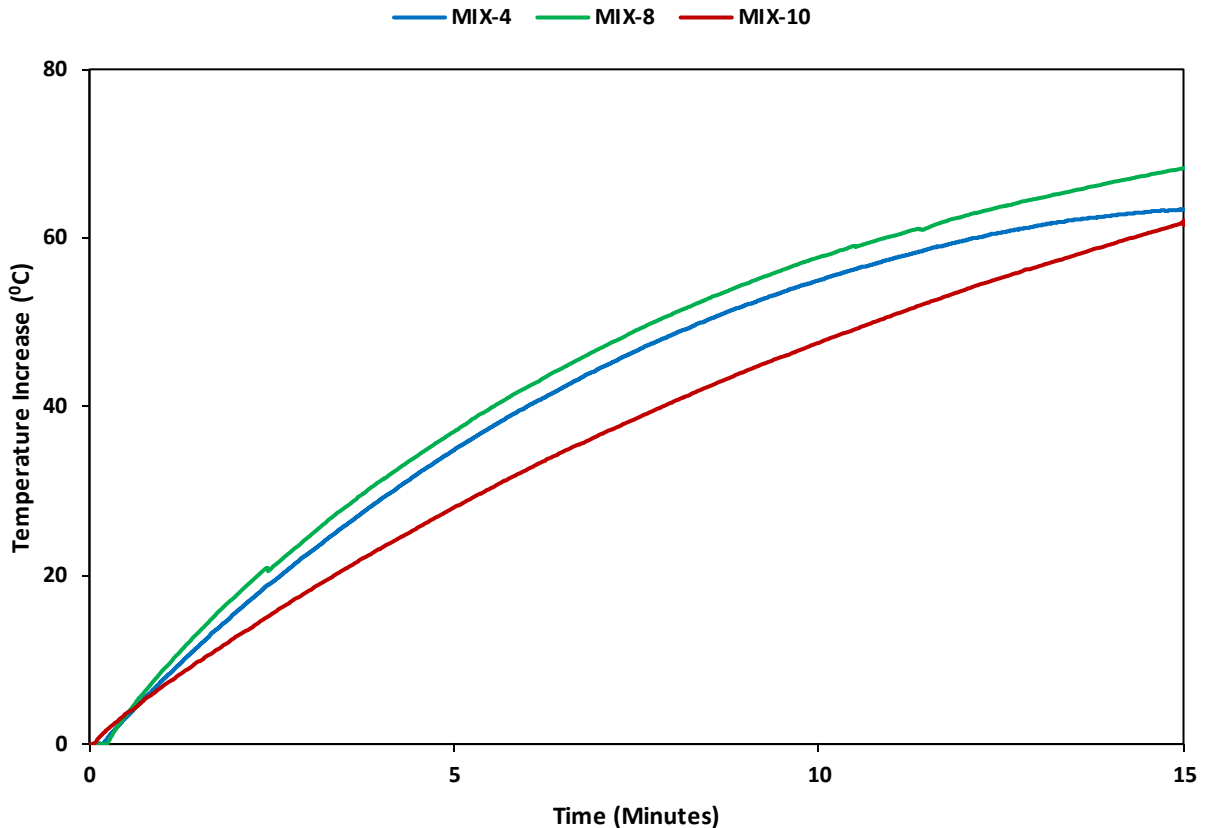


Figure 3-6 Comparison of thermal performance among different mixtures

The 28-day electrical resistivity of the Mix-8 sample was 22.72 Ω -cm. The electrical resistivity of ECON is primarily governed by the dosage rate of electrically conductive material till the percolation threshold. The percolation threshold is the dosage rate of electrically conductive material, beyond which increasing the dosage rate does not decrease the electrical resistivity by a significant amount, and for carbon fiber reinforced concrete, the percolation threshold is 1 vol.% [1]. Since the dosage rate of carbon fiber in this study was higher than 1 vol.%, lowering the carbon fiber dosage rate in the case of Mix-8 does not increase the electrical resistivity compared to Mix-1 to Mix-4. Conversely, with less carbon fiber in the mixture and a different aggregate system, Mix-8's electrical resistivity was lower than Mix-1 and similar to Mix-2 to Mix-3. For Mix-10, the electrical resistivity increased to 39 Ω -cm, although it had the

same dosage of carbon fiber as Mix-8. The difference in the aggregate source changed the aggregate system, and NMSA can be attributed to this increase in electrical resistivity of Mix-10 samples compared to Mix-8 since other variables remained similar. Therefore, beyond the carbon fiber dosage's percolation threshold zone, ECON's electrical resistivity is primarily governed by the other mixture proportioning parameters such as cement paste quantity, aggregate gradation, and aggregate system. The thermal performance of Mix-8 outperformed Mix-10, as shown in **Figure 3-6**. Although Mix-8 samples had higher electrical resistivity than Mix-4 samples, the temperature increase rate for Mix-8 samples outperformed Mix-4. The possible reason for this behavior is unknown and requires further investigation.

Conclusions

This study aimed to develop an ECON mixture procedure to produce ECON with electrical resistivity as low as possible. The key findings from this study are as follows:

1. Performance enhancement of ECON is possible by increasing the cement paste content for a given aggregate system. Workability increases with increasing cement paste content. Electrical resistivity decreases and thermal performance increases with increasing cement paste content. The increasing cement paste assisted in the fiber dispersion, but after a specific limit, no additional improvement in fiber dispersion occurred, which is why electrical resistivity did not decrease significantly after reaching a plateau.
2. The performance of ECON changes with a change in the aggregate system since the cement paste content changes with the change in the aggregate system.
3. An aggregate system with higher fine content is unsuitable for ECON production since it increases the shear stress of the mixture that is already stiff due to the presence of CF. The suitability of the aggregate system for ECON mixture changes

with NMSA and aggregate gradation changes. The aggregate system 45:10:45 (coarse: intermediate: fine) with an NMSA of 25 mm was the most suitable for the Ames source. However, a 55:45 (coarse: fine) aggregate system with 19 mm NMSA was found to be suitable for the Iowa City aggregates, according to the Power 45 and Tarantula graphs.

4. Continuous evaluation of electrical resistivity, beginning immediately after casting, is necessary to develop future electrical resistivity forecasting models.
5. Increasing cement paste does not always increase the compressive strength of ECON.
6. Beyond carbon fiber's percolation threshold, carbon fiber-reinforced ECON's performance is mainly governed by the cement paste quantity, aggregate gradation, and aggregate system. The newly developed PEM technique emphasizes the aggregate gradation and aggregate system of a mixture, and since the aggregate system controls the cement paste quantity, the PEM technique is more suitable for ECON mixture development than the ACI 211.
7. Although the VKelly index for carbon fiber-reinforced ECON was lower than the desired values or values deemed suitable for regular concrete, the ECON was still workable. Therefore, the VKelly test and interpretation of VKelly test results should be modified for fiber-reinforced concrete.

Acknowledgments

Authors gratefully acknowledge Iowa Highway Research Board (IHRB), Iowa Department of Transportation (Iowa DOT) and Federal Aviation Administration (FAA) for supporting this study. The authors would also like to express their sincere gratitude to including, but not limited to, the FAA Technical Monitors, the IHRB project technical advisory committee (TAC) members, and other participating engineers from Iowa DOT/Counties/Cities, the industry

partner, the construction contractors, the experimental material suppliers, the laboratory manager/staff in Iowa State University (ISU) Civil Engineering Department, and other research team members from ISU's Program for Sustainable Pavement Engineering & Research (PROSPER) and National Concrete Pavement Technology Center (CP Tech Center) at the InTrans for their support and assistance. Although the IHRB, Iowa DOT, and FAA have sponsored this study, they neither endorse nor reject any comments made in this paper. The presentation of this information is in the interest of invoking comments by the technical community with respect to the results and conclusions of the research. This paper does not constitute a standard, specification, or regulation.

References

- [1] M.L. Rahman, A. Malakooti, H. Ceylan, S. Kim, P.C. Taylor, A review of electrically conductive concrete heated pavement system technology: From the laboratory to the full-scale implementation, *Constr. Build. Mater.* 329 (2022) 127139. <https://doi.org/10.1016/j.conbuildmat.2022.127139>.
- [2] A. Malakooti, H. Abdulla, S. Sadati, H. Ceylan, S. Kim, K. Cetin, Experimental and theoretical characterization of electrodes on electrical and thermal performance of electrically conductive concrete, *Compos. Part B Eng.* 222 (2021) 109003. <https://doi.org/10.1016/j.compositesb.2021.109003>.
- [3] H. Abdulla, H. Ceylan, S. Kim, K. Gopalakrishnan, P.C. Taylor, Y. Turkan, System requirements for electrically conductive concrete heated pavements, *Transp. Res. Rec.* 2569 (2016) 70–79. <https://doi.org/10.3141/2569-08>.

- [4] L. Sutter, K. Peterson, G. Julio-Betancourt, D. Hooton, T. Van Van Dam, K. Smith, The deleterious chemical effects of concentrated deicing solutions on Portland cement concrete, 2008.
http://www.michiganltap.org/sites/ltap/files/workshops/materials/a_darker_side_of_anti_icing_chemicals.pdf.
- [5] W.M. Lewis, Studies of Environmental Effects of Magnesium Chloride Deicer in Colorado, 1999. file:///C:/Users/Owner/Downloads/1999-10.pdf.
- [6] A. Sassani, H. Ceylan, S. Kim, A. Arabzadeh, P.C. Taylor, K. Gopalakrishnan, Development of Carbon Fiber-modified Electrically Conductive Concrete for Implementation in Des Moines International Airport, Case Stud. Constr. Mater. 8 (2018) 277–291.
<https://doi.org/10.1016/j.cscm.2018.02.003>.
- [7] A. Malakooti, W.S. Theh, S.M.S. Sadati, H. Ceylan, S. Kim, M. Mina, K. Cetin, P.C. Taylor, Design and Full-scale Implementation of the Largest Operational Electrically Conductive Concrete Heated Pavement System, Constr. Build. Mater. 255 (2020) 119229.
<https://doi.org/10.1016/j.conbuildmat.2020.119229>.
- [8] E. Yurdakul, Proportioning for performance-based concrete pavement mixtures, PhD. Thesis. (2013) 227.
- [9] H. Abdulla, H. Ceylan, S. Kim, M. Mina, K.S. Cetin, P.C. Taylor, K. Gopalakrishnan, B. Cetin, S. Yang, A. Vidyadharan, Design and Construction of the World's First Full-Scale Electrically Conductive Concrete Heated Airport Pavement System at a U.S. Airport, Transp. Res. Rec. 2672 (2018) 82–94. <https://doi.org/10.1177/0361198118791624>.
- [10] X. Wang, P. Taylor, E. Yurdakul, X. Wang, An innovative approach to concrete mixture proportioning, ACI Mater. J. 115 (2018) 749–759. <https://doi.org/10.14359/51702351>.

[11] E. Yurdakul, P.C. Taylor, H. Ceylan, F. Bektas, Effect of Paste-to-Voids Volume Ratio on the Performance of Concrete Mixtures, *J. Mater. Civ. Eng.* 25 (2013) 1840–1851.

[https://doi.org/10.1061/\(asce\)mt.1943-5533.0000728](https://doi.org/10.1061/(asce)mt.1943-5533.0000728).

[12] X. Wang, P. Taylor, X. Wang, Using a Vibrating Kelly Ball Test (VKelly Test) to Determine the Workability of Slipform Concrete Mixtures, *DEStech Trans. Eng. Technol. Res.*

(2017). <https://doi.org/10.12783/dtetr/ictim2016/5599>.

[13] L. Struble, R. Szecsy, W.-G. Lei, G.-K. Sun, Rheology of cement paste and concrete, *Cem. Concr. Aggregates*. 20 (1998).

CHAPTER 4. GENERAL CONCLUSIONS

This thesis identified challenges ahead for full-scale ECON HPS implementation by critically reviewing the existing literature on this technology and discussing ways to address those challenges.

State of the art and contribution to engineering research

The overall contribution of this study to engineering research is:

- Carbon and steel fibers are commonly incorporated into concrete to enhance electrical conductivity. Additionally, materials like Carbon Nanofibers, Carbon Nanotubes, graphite, carbon black, and steel shavings have proven effective in increasing the electrical conductivity of concrete.
- Successful implementation of full-scale ECON HPS technology faces several challenges, including initial construction costs, ensuring consistent construction quality when moving between laboratory and field-scale ECON production, establishing proper design and construction specifications, adapting ECON for frigid weather conditions (temperatures below -25°C) while addressing safety concerns.
- ECON HPS technology includes an electrically conductive concrete layer, embedded electrodes, a power supply, sensors, and a control system.
- Beyond its use as a heated pavement layer, ECON can find applications in Ohmic heat curing of concrete and indoor radiant heating technology.
- Improving ECON performance is achievable by increasing the cement paste content within a given aggregate system, resulting in improved workability, reduced electrical resistivity, and enhanced thermal performance. However, electrical resistivity does

not decrease significantly after reaching a certain point due to limitations in fiber dispersion.

- Since altering the aggregate system leads to changes in the cement paste content, ECON's performance is affected by changes in the aggregate system. An aggregate system with a high fine content is unsuitable for ECON production because it further stiffens the carbon fibers mixture. The suitability of an aggregate system for use in ECON varies with the Nominal Maximum Size of Aggregate (NMSA) and changes in aggregate gradation. For example, a 45:10:45 (coarse: intermediate: fine) aggregate system with a 25 mm NMSA was the most suitable for the Ames source. However, based on the Power 45 and Tarantula graphs, a 55:45 (coarse: fine) aggregate system with a 19 mm NMSA was deemed suitable for Iowa City aggregates.
- Continuous monitoring of electrical resistivity immediately after casting is essential for developing future electrical resistivity forecasting models.
- It is important to note that an increase in cement paste content does not always lead to a corresponding increase in the compressive strength of ECON.
- Beyond the carbon fiber percolation threshold, carbon-fiber-reinforced ECON's performance is primarily influenced by the quantity of cement paste, aggregate gradation, and the chosen aggregate system. The newly developed PEM technique emphasizes aggregate gradation and the aggregate system, and since the aggregate system controls cement paste quantity, the PEM technique is more suitable than the ACI 211 method for developing ECON mixtures.

- Even though its VKelly index for carbon fiber-reinforced ECON may fall below-desired values or values considered suitable for regular concrete, an ECON mixture remains workable, so the VKelly test and its interpretation remain relevant.

Recommendations for Future Studies

Future studies should focus on:

- Identifying cost-effective electrically-conductive materials to mitigate the initial construction costs associated with ECON. Since the addition of electrically conductive materials is a primary contributor to increased construction expenses of ECON HPS compared to conventional pavements, integrating more economical materials into the concrete mixture can significantly reduce the costs of this pavement type.
- Establishing correlations between performance and design parameters for ECON HPS. Since the key performance parameter to consider is the rate of temperature increase, it is advisable to develop correlations between the rate of temperature increase and various design parameters of ECON HPS, including electrical resistivity of ECON, electrode size, spacing, placement depth, and applied voltage levels. These equations can then be seamlessly integrated into the design processes for ECON HPS.
- It is essential to create comprehensive construction guidelines and specifications that will enable relevant agencies to incorporate this innovative pavement technology into their road systems efficiently.
- Rehabilitation of ECON heated pavement is an area that remains unexplored by researchers. Future research should identify potential types of distress that can affect this

type of pavement and formulate effective rehabilitation plans to enhance the lifespan of this pavement type, resulting in a more favorable benefit-to-cost ratio.

As climate dynamics continue to evolve, the significance of resilient winter maintenance practices in transportation infrastructure cannot be overstated. Proactively addressing the challenges associated with ECON HPS allows us to transition towards more cost-effective, eco-friendly, and sustainable solutions, benefiting the transportation industry and the environment. Doing so will make it possible to ensure transportation networks' continued functionality and safety in frigid climates, ultimately fostering economic growth and safeguarding the public's well-being.